

Deviations from Geodesic Evolutions and Energy Waste on the Bloch Sphere

Leonardo Rossetti^{1,2}, Carlo Cafaro^{2,3}, Paul M. Alsing²

¹University of Camerino, I-62032 Camerino, Italy

²University at Albany-SUNY, Albany, NY 12222, USA and

³SUNY Polytechnic Institute, Utica, NY 13502, USA

In optimal quantum-mechanical evolutions, motion can occur along non-predetermined paths of shortest length in an optimal time. Alternatively, optimal evolutions can happen along predefined paths with no waste of energy resources and 100% speed efficiency. Unfortunately, realistic physical scenarios typically result in less-than-ideal evolutions. In this paper, we study different families of sub-optimal qubit Hamiltonians, both stationary and time-varying, for which the so-called geodesic efficiency and the speed efficiency of the corresponding quantum evolutions are less than one. Furthermore, after proposing an alternative hybrid efficiency measure constructed out of the two previously mentioned efficiency quantifiers, we provide illustrative examples where the average departures from time-optimality and 100% speed efficiency are globally captured over a limited time period. In particular, thanks to this hybrid measure, quantum evolutions are partitioned in four categories: Geodesic unswasteful, nongeodesic unswasteful, geodesic wasteful and, lastly, nongeodesic wasteful. Finally, we discuss Hamiltonians specified by magnetic field configurations, both stationary and nonstationary, yielding optimal hybrid efficiency (that is, both time-optimality and 100% speed efficiency) over a finite time interval.

PACS numbers: Quantum Computation (03.67.Lx), Quantum Information (03.67.Ac), Quantum Mechanics (03.65.-w), Riemannian Geometry (02.40.Ky).

I. INTRODUCTION

Background. It is known that geometric reasoning can be very insightful in quantum physics [1]. For instance, the geometry of quantum states can be exploited to specify our restricted capacity in discriminating one quantum state, either pure or mixed, from another by means of experimental observations [2–8]. In practical scenarios specified by departures from ideal conditions, the effective quantum-mechanical evolution of a physical system may not be described by the geometry on the space of quantum states.

First, practical scenarios may not always be specified by evolutions that occur along the shortest paths, as realistic quantum dynamics evolution could potentially follow longer paths of evolution due to the presence of possible imperfections. For instance, not all Hamiltonian evolutions between an initial and a final pure quantum state yield shortest time evolutions that occur with optimal speed along the shortest path connecting a source and a target state [9–20]. For this reason, the actual paths followed by points in projective Hilbert spaces during quantum dynamics are not the same as the geodesic paths on the underlying quantum state space with an appropriate metric (e.g., for pure states, the projective Hilbert space with the Fubini-Study metric). When focusing on pure states, we can identify Hamiltonian operators that drive quantum evolutions at the fastest possible rate [15, 16]. These quantum dynamical trajectories, known as Hamiltonian curves, follow geodesic paths on the metricized manifolds of quantum states, as states evolve according to specific physical evolutions. A main quantity used to quantify the departure from the ideal geodesic evolution on a manifold of pure states is the so-called geodesic efficiency η_{GE} proposed by Anandan and Aharonov in Ref. [9]. This quantity is a global quantifier since it is evaluated over a finite temporal interval. It is defined in terms of the ratio between two lengths, s_0 and s . The quantity s_0 denotes the geodesic distance, that is, the length of the shortest path between the initial and final states ($|A\rangle$ and $|B\rangle$, respectively) measured with respect to the Fubini-Study metric (where $s_0 = 2s_{\text{FS}}$, with s_{FS} being the Fubini-Study distance). The quantity s , instead, denotes the length of the actual path followed by the quantum system. In particular, s depends on the energy uncertainty of the system governed by a stationary or time-varying Hamiltonian.

Second, practical scenarios may not always be energy-efficient and could result in some energy wastage. Indeed, instead of minimizing the length of a non pre-defined path connecting two states, one may be interested in minimizing the waste of energy resources directly used for the motion of the quantum system on a pre-defined path in complex projective Hilbert space [21–24]. In this respect, a key quantity employed to characterize the effective amount of energy used by the system for evolving with 100% evolution speed is the so-called speed efficiency introduced by Uzdin and collaborators in Ref. [21]. This quantity is a local quantifier since it is defined at each instant in time. It can be expressed as the ratio between two energies, the energy uncertainty ΔE of the system (i.e., the square root of the variance of the generally time-varying Hamiltonian operator) and the spectral norm $\|H\|_{\text{SP}}$ of the Hamiltonian operator that specifies the dynamics.

Physical Motivation. Considering the information we have presented up to this point, it is clear that the transition of

a quantum system from an initial source state to a final target state in the minimal time possible, while simultaneously minimizing energy expenditure, is critically significant in the realm of quantum information processing. Typically, the time-optimality of quantum evolution is assessed through the notion of geodesic efficiency, whereas the energy resources expended during this evolution are evaluated using the concept of speed efficiency. Additionally, time-optimality can be defined by examining the progression of the quantum system along a non-predetermined trajectory in projective Hilbert space over a finite duration, utilizing a “global” measure such as geodesic efficiency. Conversely, the least amount of energy expended can be assessed in real-time via a “local” measure like the speed efficiency while observing the quantum system as it progresses along a specified path in projective space. To ensure clarity in the discussion, consider a two-level quantum system as a spin-1/2 particle subjected to an external magnetic field. Then, it is essential to recognize that optimal ideal conditions for achieving unit geodesic and speed efficiencies necessitate particular configurations of the magnetic field corresponding to a specified initial source state on the Bloch sphere. Furthermore, it is imperative that the magnetic field remains free from any imperfections.

Physics is inherently an experimental discipline characterized by the prevalence of approximations and imperfections. Specifically, minor discrepancies in magnetic fields, both in terms of strength and orientation, are often unavoidable in laboratory settings [25]. For example, researchers utilize magnetic fields produced by superconducting magnets within a cyclotron to direct charged particles along intricate trajectories while maintaining their velocity, as well as to identify these particles by observing their deflection in the presence of the magnetic field [25–28]. However, any misalignment of the magnets may result in alterations to the magnetic field profile. Such alterations can subsequently lead to instabilities in the specified particle trajectories, potentially causing deviations from the shortest paths along with loss of speed.

Driven by these physical considerations, our objective is to leverage geodesic and speed efficiencies to introduce a concept of hybrid efficiency for quantum evolutions on the Bloch sphere. This concept aims to quantify both the deviations from geodesic trajectories and the expenditure of energy resources over a specified duration.

Goals and Relevance. From an intuitive standpoint, it is clear that geodesic efficiency and speed efficiency capture distinct aspects of a quantum evolution. In particular, it seems reasonable to expect that one would be naturally interested in achieving both time-optimality (at a global level) and 100% speed efficiency (at a local level). However, to understand how one can achieve these two ideal goals, it is important to tackle two main points. First, one needs to construct suitable families of optimal and suboptimal quantum evolutions that connect the same quantum states. Second, one has to gain helpful physical insights on the nature of the distinct aspects captured by these two different optimality measures for quantum evolutions. Therefore, it is the subject of this paper that of tackling these two relevant points. Our goal is to address an array of queries, such as:

- [i] How does a time-dependent magnetic field configuration (specifically, parallel and transverse magnetic field components with respect to the evolving Bloch vector) change the geodesic and speed efficiencies of a quantum evolution?
- [ii] Can we quantify quantum evolutions that occur over a finite time interval in terms of both time-optimality and minimum waste of energy resources by means of a sort of hybrid efficiency measure? How can we conveniently define such a measure?
- [iii] Can we identify suitable time-varying magnetic field configurations capable of yielding an optimal hybrid efficiency for a quantum evolution?

The discussion of points [i], [ii], and [iii] holds significant importance in the realm of quantum information and computation for various reasons. Specifically, a thorough quantitative comprehension of these aspects can facilitate the creation of effective quantum control strategies that enable the efficient transfer of a source state to a target state, achieving this in the least amount of time, at optimal velocity, and with minimal energy expenditure. Moreover, we anticipate that our hybrid efficiency measure will prove particularly beneficial in realistic situations where a decision must be made between optimizing time efficiency or minimizing energy loss, depending on the acceptable levels of time or energy loss that can be tolerated in actual experimental settings. Finally, from a theoretical standpoint, we have reason to believe that this measure may enhance our understanding of the curvature [29] and complexity [30] of quantum evolutions. For clarity, lastly, we would like to emphasize that the research detailed in Ref. [29] and the study presented in this paper are complementary yet separate endeavors, as they address different subjects.

Prior to outlining the structure of this paper, it is important to emphasize that the terms “time-dependent, time-varying, and nonstationary” Hamiltonian evolutions (or, conversely, magnetic field configurations) are utilized interchangeably throughout this study.

The layout of the rest of the paper is as follows. In Section II, after reviewing the concepts of geodesic and speed efficiencies, we propose a hybrid efficiency measure η_{HE} suitable for capturing the average departures from time-optimality and 100% speed efficiency. In Section III, we construct a one-parameter family of stationary qubit

Hamiltonians connecting two states $|A\rangle$ and $|B\rangle$ along nongeodesic paths on the Bloch sphere. Furthermore, we analyze both non-traceless and traceless time-varying Hamiltonians yielding energy-wasteful evolutions. In both cases, we characterize the evolutions in terms of the geodesic and speed efficiencies. In Section IV, we use the formalism introduced in the previous section to present four illustrative examples. Specifically, we describe the full spectrum of possible quantum evolutions: Geodesic unwasteful, geodesic wasteful, nongeodesic wasteful and, finally, nongeodesic unwasteful evolutions. In all cases, we quantify the average properties of the quantum motion in terms of the newly proposed hybrid efficiency measure. In Section V, we present a summary of results together with some final remarks. Finally, technical details are placed in Appendixes A and B.

II. EFFICIENCY MEASURES

In this section, after recalling the concepts of geodesic [9, 31] and speed [21] efficiencies, we propose a hybrid efficiency measure suitable for capturing the average departures from time-optimality and 100% speed efficiency. In what follows, we limit our discussion to the physics of two-level quantum systems described by pure states that evolve under arbitrary Hermitian evolutions.

A. Geodesic efficiency

We begin by recalling the notion of geodesic efficiency for a quantum evolution as originally introduced by Anandan and Aharonov in Ref. [9]. Take into consideration an evolution of a state vector $|\psi(t)\rangle$ characterized by the time-dependent Schrödinger equation, $i\hbar\partial_t|\psi(t)\rangle = H(t)|\psi(t)\rangle$, with $t_A \leq t \leq t_B$. While this introductory presentation presupposes that the reduced Planck constant, denoted as \hbar , is not equal to one, we will adopt the convention of setting $\hbar = 1$ for the majority of our explicit calculations throughout this paper. We will make it a point to remind the reader of this choice whenever it is deemed necessary. Then, the geodesic efficiency η_{GE} for such a quantum evolution is a time-independent (global) scalar quantity with $0 \leq \eta_{\text{GE}} \leq 1$ defined as [9, 31]

$$\eta_{\text{GE}} \stackrel{\text{def}}{=} \frac{s_0}{s} = 1 - \frac{\Delta s}{s} = \frac{2 \arccos[|\langle A|B\rangle|]}{2 \int_{t_A}^{t_B} \frac{\Delta E(t)}{\hbar} dt}, \quad (1)$$

with $\Delta s \stackrel{\text{def}}{=} s - s_0$. The quantity s_0 was mentioned in the Introduction and denotes the distance along the shortest geodesic path that joins the initial $|A\rangle \stackrel{\text{def}}{=} |\psi(t_A)\rangle$ and final $|B\rangle \stackrel{\text{def}}{=} |\psi(t_B)\rangle$ states on the complex projective Hilbert space. Moreover, as briefly pointed out in our Introduction, the quantity s in Eq. (1) is the distance along the dynamical trajectory $\gamma(t) : t \mapsto |\psi(t)\rangle$ corresponding to the evolution of the state vector $|\psi(t)\rangle$ with $t_A \leq t \leq t_B$. Obviously, a geodesic quantum evolution with $\gamma(t) = \gamma_{\text{geodesic}}(t)$ is defined by the relation $\eta_{\text{GE}}^{\gamma_{\text{geodesic}}} = 1$. Focusing on the numerator in Eq. (1), we note that it defines the angle between the unit state vectors $|A\rangle$ and $|B\rangle$ and equals the Wootters distance [3]. Specifically, setting $\rho_A \stackrel{\text{def}}{=} |A\rangle\langle A| = (\mathbf{1} + \hat{a} \cdot \boldsymbol{\sigma})/2$ and $\rho_B \stackrel{\text{def}}{=} |B\rangle\langle B| = (\mathbf{1} + \hat{b} \cdot \boldsymbol{\sigma})/2$ with unit vectors \hat{a} and \hat{b} such that $\hat{a} \cdot \hat{b} = \cos(\theta_{AB})$, it happens that $s_0 = \theta_{AB}$ since $|\langle A|B\rangle|^2 = \text{tr}(\rho_A \rho_B) + 2\sqrt{\det(\rho_A) \det(\rho_B)} = (1 + \hat{a} \cdot \hat{b})/2 = \cos^2(\theta_{AB}/2)$. Clearly, $\boldsymbol{\sigma} \stackrel{\text{def}}{=} (\sigma_x, \sigma_y, \sigma_z)$ is the vector operator specified by the usual Pauli operators. The denominator in Eq. (1), instead, specifies the integral of the infinitesimal distance $ds \stackrel{\text{def}}{=} 2[\Delta E(t)/\hbar] dt$ along the evolution curve in ray space [9]. The quantity $\Delta E(t) \stackrel{\text{def}}{=} \left[\langle \psi | H^2(t) | \psi \rangle - \langle \psi | H(t) | \psi \rangle^2 \right]^{1/2}$ is the energy uncertainty of the system expressed as the square root of the dispersion of $H(t)$. Notably, Anandan and Aharonov showed that the infinitesimal distance $ds \stackrel{\text{def}}{=} 2[\Delta E(t)/\hbar] dt$ is connected to the Fubini-Study infinitesimal distance ds_{FS} via the relation [9],

$$ds_{\text{FS}}^2(|\psi(t)\rangle, |\psi(t+dt)\rangle) \stackrel{\text{def}}{=} 4 \left[1 - |\langle \psi(t) | \psi(t+dt) \rangle|^2 \right] = 4 \frac{\Delta E^2(t)}{\hbar^2} dt^2 + \mathcal{O}(dt^3), \quad (2)$$

where $\mathcal{O}(dt^3)$ specifies an infinitesimal quantity of order equal to or higher than dt^3 . From the connection between ds_{FS} and ds , one arrives at the conclusion that s is proportional to the time integral of ΔE . Moreover, s defines the distance measured by the Fubini-Study metric along the evolution of the quantum system in ray space. We stress that, when the actual dynamical curve is the shortest geodesic path joining $|A\rangle$ and $|B\rangle$, Δs equals zero and the geodesic efficiency η_{GE} in Eq. (1) becomes one. Clearly, π is the shortest possible distance between two orthogonal pure states in ray space. Before moving to the speed efficiency, we note that if we set $H(t) \stackrel{\text{def}}{=} h_0(t) \mathbf{1} + \mathbf{h}(t) \cdot \boldsymbol{\sigma}$

and $\rho(t) \stackrel{\text{def}}{=} (\mathbf{1} + \hat{a}(t) \cdot \boldsymbol{\sigma})/2$ with $t_A \leq t \leq t_B$, the energy uncertainty $\Delta E(t) \stackrel{\text{def}}{=} \sqrt{\text{tr}(\rho H^2) - [\text{tr}(\rho H)]^2}$ reduces to $\Delta E(t) = \sqrt{\mathbf{h}^2 - [\hat{a}(t) \cdot \mathbf{h}]^2}$. Finally, the geodesic efficiency in Eq. (1) can be recast as

$$\eta_{\text{GE}} = \frac{2 \arccos\left(\sqrt{\frac{1 + \hat{a} \cdot \hat{b}}{2}}\right)}{\int_{t_A}^{t_B} \frac{2}{\hbar} \sqrt{\mathbf{h}^2 - [\hat{a}(t) \cdot \mathbf{h}]^2} dt}, \quad (3)$$

with $\hat{a}(t_A) \stackrel{\text{def}}{=} \hat{a}$ and $\hat{a}(t_B) = \hat{b}$ in Eq. (3). Interestingly, for $\mathbf{H}(t) \stackrel{\text{def}}{=} \mathbf{h}(t) \cdot \boldsymbol{\sigma}$ and setting

$$\mathbf{h} = [\mathbf{h} \cdot \hat{a}] \hat{a} + [\mathbf{h} - (\mathbf{h} \cdot \hat{a})\hat{a}] = \mathbf{h}_{\parallel} + \mathbf{h}_{\perp}, \quad (4)$$

where $\hat{a} = \hat{a}(t)$ in the decomposition of \mathbf{h} , η_{GE} in Eq. (3) reduces to

$$\eta_{\text{GE}} = \frac{\arccos\left(\sqrt{\frac{1 + \hat{a} \cdot \hat{b}}{2}}\right)}{\int_{t_A}^{t_B} h_{\perp}(t) dt}. \quad (5)$$

Therefore, from Eq. (5) one can see that η_{GE} depends only on $h_{\perp}(t)$. Intriguingly, keeping $\hbar = 1$, we note that Feynman's geometric evolution equation [1] $d\hat{a}/dt = 2\mathbf{h} \times \hat{a}$ for the time-dependent unit Bloch vector $\hat{a} = \hat{a}(t)$ can be viewed as a local formulation of the Anandan-Aharonov relation $s = \int 2\Delta E(t) dt$. Indeed, from $d\hat{a}/dt = 2\mathbf{h} \times \hat{a}$, we get $da^2 = 4h_{\perp}^2 dt^2$. Similarly, from $s = \int 2\Delta E(t) dt$, we obtain $ds = 2h_{\perp} dt$. Therefore, combining these two differential relations, we finally get $da = 2h_{\perp} dt = ds$.

We can now discuss the notion of speed efficiency.

B. Speed efficiency

In Ref. [21], Uzdin *et al.* proposed appropriate families of nonstationary Hamiltonians capable of generating predetermined dynamical trajectories characterized by a minimal waste of energy resources. These trajectories, although being energetically resourceful, are not generally geodesic paths of minimum length. Specifically, the constraint of minimal waste of energetic resources is obtained when no energy is wasted on portions of the Hamiltonian that do not effectively steer the system. Put differently, all the available energy described by the spectral norm of the Hamiltonian $\|\mathbf{H}\|_{\text{SP}}$ is transformed into the speed of evolution of the system $v_{\text{H}}(t) \stackrel{\text{def}}{=} (2/\hbar)\Delta E(t)$ with $\Delta E(t)$ being the energy uncertainty. More explicitly, the so-called Uzdin's speed efficiency η_{SE} is a time-dependent (local) scalar quantity with $0 \leq \eta_{\text{SE}} \leq 1$ given by [21]

$$\eta_{\text{SE}} \stackrel{\text{def}}{=} \frac{\Delta H_{\rho}}{\|\mathbf{H}\|_{\text{SP}}} = \frac{\sqrt{\text{tr}(\rho H^2) - [\text{tr}(\rho H)]^2}}{\max\left[\sqrt{\text{eig}(\mathbf{H}^{\dagger}\mathbf{H})}\right]}. \quad (6)$$

While $\rho = \rho(t)$ is the density operator that describes the quantum system at time t , the quantity $\|\mathbf{H}\|_{\text{SP}}$ in the denominator of Eq. (6) is defined as $\|\mathbf{H}\|_{\text{SP}} \stackrel{\text{def}}{=} \max\left[\sqrt{\text{eig}(\mathbf{H}^{\dagger}\mathbf{H})}\right]$. It is the so-called spectral norm $\|\mathbf{H}\|_{\text{SP}}$ of the Hamiltonian operator \mathbf{H} which is a measure of the size of bounded linear operators. It is expressed as the square root of the maximum eigenvalue of the operator $\mathbf{H}^{\dagger}\mathbf{H}$, where \mathbf{H}^{\dagger} denotes the Hermitian conjugate of \mathbf{H} . Focusing on two-level quantum systems and assuming the nonstationary Hamiltonian in Eq. (6) to be given by $\mathbf{H}(t) \stackrel{\text{def}}{=} h_0(t) \mathbf{1} + \mathbf{h}(t) \cdot \boldsymbol{\sigma}$, we observe that the speed efficiency η_{SE} in Eq. (6) can be conveniently expressed as

$$\eta_{\text{SE}} = \eta_{\text{SE}}(t) \stackrel{\text{def}}{=} \frac{\sqrt{\mathbf{h}^2 - (\hat{a} \cdot \mathbf{h})^2}}{|h_0| + \sqrt{\mathbf{h}^2}}. \quad (7)$$

While $\hat{a} = \hat{a}(t)$ in Eq. (7) is the instantaneous unit Bloch vector that describes the qubit state of the system, the set $\text{eig}(\mathbf{H}^{\dagger}\mathbf{H})$ in the definition of $\|\mathbf{H}\|_{\text{SP}}$ equals

$$\text{eig}(\mathbf{H}^{\dagger}\mathbf{H}) = \left\{ \lambda_{\mathbf{H}^{\dagger}\mathbf{H}}^{(+)} \stackrel{\text{def}}{=} (h_0 + \sqrt{\mathbf{h}^2})^2, \lambda_{\mathbf{H}^{\dagger}\mathbf{H}}^{(-)} \stackrel{\text{def}}{=} (h_0 - \sqrt{\mathbf{h}^2})^2 \right\}. \quad (8)$$

Type of scenario	$\bar{\eta}_{\text{GE}}$	$\bar{\eta}_{\text{SE}}$	η_{HE}	Type of quantum evolution
First	1	1	1	Geodesic unwasteful
Second	< 1	1	< 1	Nongeodesic unwasteful
Third	1	< 1	< 1	Geodesic wasteful
Fourth, first subcase	< 1	$\ll 1$	$\ll 1$	More wasteful than nongeodesic
Fourth, second subcase	$\ll 1$	< 1	$\ll 1$	Less wasteful than nongeodesic
Fourth, third subcase	< 1	< 1	< 1	As wasteful as nongeodesic

TABLE I: Schematic summary of the variety of scenarios for quantum evolutions in terms of the average departure from geodesic motion (quantified by the average geodesic efficiency $\bar{\eta}_{\text{GE}}$ over $[t_A, t_B]$) and of the average deviation from minimally energy wasteful evolutions (quantified by the average speed efficiency $\bar{\eta}_{\text{SE}}$ over $[t_A, t_B]$). Finally, the hybrid efficiency η_{HE} is given by $\eta_{\text{HE}} \stackrel{\text{def}}{=} \bar{\eta}_{\text{GE}} \cdot \bar{\eta}_{\text{SE}}$.

Notice that since the eigenvalues of $\mathbf{H}(t) \stackrel{\text{def}}{=} h_0(t) \mathbf{1} + \mathbf{h}(t) \cdot \boldsymbol{\sigma}$ are $E_{\pm} \stackrel{\text{def}}{=} h_0 \pm \sqrt{\mathbf{h} \cdot \mathbf{h}}$, the quantity $h_0 = (E_+ + E_-)/2$ represents the average of the two energy levels. Furthermore, $\sqrt{\mathbf{h}^2} = (E_+ - E_-)/2$ is proportional to the energy splitting $E_+ - E_-$ between the two energy levels E_{\pm} with $E_+ \geq E_-$. Finally, for a trace zero time-dependent Hamiltonian $\mathbf{H}(t) \stackrel{\text{def}}{=} \mathbf{h}(t) \cdot \boldsymbol{\sigma}$ for which $\hat{a}(t) \cdot \mathbf{h}(t) = 0$ for any temporal instant t , the speed efficiency $\eta_{\text{SE}}(t)$ is equal to one. Thus, the quantum evolution happens with no waste of energy resources. Interestingly, for $\mathbf{H}(t) \stackrel{\text{def}}{=} \mathbf{h}(t) \cdot \boldsymbol{\sigma}$ and setting $\mathbf{h} = (\mathbf{h} \cdot \hat{a})\hat{a} + [\mathbf{h} - (\mathbf{h} \cdot \hat{a})\hat{a}] = \mathbf{h}_{\parallel} + \mathbf{h}_{\perp}$ with $\mathbf{h}_{\parallel} \cdot \mathbf{h}_{\perp} = 0$, $\eta_{\text{SE}}(t)$ in Eq. (7) can be completely expressed in term of the parallel (i.e., $\mathbf{h}_{\parallel} \stackrel{\text{def}}{=} h_{\parallel} \hat{h}_{\parallel}$) and transverse (i.e., $\mathbf{h}_{\perp} \stackrel{\text{def}}{=} h_{\perp} \hat{h}_{\perp}$) components of the “magnetic” field vector \mathbf{h} as

$$\eta_{\text{SE}}(t) = \frac{h_{\perp}(t)}{\sqrt{h_{\perp}^2(t) + h_{\parallel}^2(t)}}. \quad (9)$$

From Eq. (9), it is evident that $\eta_{\text{SE}}(t) = 1$ if and only if $h_{\parallel}(t) = 0$ for any t . In other words, if and only if $\hat{a}(t) \cdot \mathbf{h}(t) = 0$ for any t .

Limiting our attention to qubit systems, we point out for completeness that Hamiltonians $\mathbf{H}(t)$ in Ref. [21], which give unit speed efficiency trajectories, are proposed so that they give rise to the same motion $\pi(|\psi(t)\rangle)$ in the complex projective Hilbert space $\mathbb{C}P^1$ (or, alternatively, on the Bloch sphere $S^2 \cong \mathbb{C}P^1$) as $|\psi(t)\rangle$. The projection operator π can be formally defined in terms of $\pi : \mathcal{H}_2^1 \ni |\psi(t)\rangle \mapsto \pi(|\psi(t)\rangle) \in \mathbb{C}P^1$. It can be demonstrated that an Hamiltonian $\mathbf{H}(t)$ of this kind can be expressed as [21]

$$\mathbf{H}(t) = i |\partial_t m(t)\rangle \langle m(t)| - i |m(t)\rangle \langle \partial_t m(t)|, \quad (10)$$

where, for ease of notation, we can put $|m(t)\rangle = |m\rangle$ and $|\partial_t m(t)\rangle = |\partial_t m\rangle = \partial_t |m\rangle = |\dot{m}\rangle$. The state $|m\rangle$ satisfies $\pi(|m(t)\rangle) = \pi(|\psi(t)\rangle)$, $i\partial_t |m(t)\rangle = \mathbf{H}(t) |m(t)\rangle$, and $\eta_{\text{SE}}(t) = 1$. The constraint $\pi(|m(t)\rangle) = \pi(|\psi(t)\rangle)$ entails that $|m(t)\rangle = c(t) |\psi(t)\rangle$, with $c(t)$ being a complex scalar function. Requiring that $\langle m|m\rangle = 1$, we obtain $|c(t)| = 1$. Therefore, $c(t)$ can be recast as $e^{i\phi(t)}$ with the phase $\phi(t) \in \mathbb{R}$. Then, enforcing the parallel transport condition $\langle m|\dot{m}\rangle = \langle \dot{m}|m\rangle = 0$, the phase $\phi(t)$ reduces to $i \int \langle \psi|\dot{\psi}\rangle dt$. Therefore, the state $|m(t)\rangle$ becomes $|m(t)\rangle = \exp(-\int_0^t \langle \psi(t')|\partial_{t'} \psi(t')\rangle dt') |\psi(t)\rangle$. Observe that the Hamiltonian $\mathbf{H}(t)$ in Eq. (10) has trace zero by construction given that its matrix representation with respect to the in the orthogonal basis $\{|m\rangle, |\partial_t m\rangle\}$ has only off-diagonal elements. Moreover, the equation $i\partial_t |m(t)\rangle = \mathbf{H}(t) |m(t)\rangle$ suggests that $|m(t)\rangle$ fulfils the time-dependent Schrödinger evolution equation. Lastly, the condition $\eta_{\text{SE}}(t) = 1$ means that $\mathbf{H}(t)$ steers the state $|m(t)\rangle$ with maximal speed and no waste of energetic resources.

Having recalled the notions of geodesic and speed efficiencies, we are now ready to propose our hybrid efficiency measure.

C. Hybrid efficiency

In what follows, we focus on single-qubit quantum Hamiltonian evolutions on the Bloch sphere. We have discussed two distinct efficiency measures of quantum evolutions. The first measure, called *geodesic efficiency* $\eta_{\text{GE}} \stackrel{\text{def}}{=} s_0/s$, specifies the departure of the actual quantum path of length s connecting two given unit quantum states $|A\rangle$ and $|B\rangle$

from the ideal geodesic path of length s_0 . The concept of length of a path, be it s_0 calculated using the Fubini-Study metric or s calculated according to the Anandan-Aharonov prescription, is the key notion in the definition of η_{GE} . Therefore, the shortest path connecting two pre-defined quantum states is the maximally efficient according to η_{GE} . When using η_{GE} , we can only speak of geodesic or nongeodesic quantum evolutions that occur during a temporal interval of length $t_B - t_A$. It does not make sense to speak of the geodesic efficiency at given instant in time. The efficiency η_{GE} is not an instantaneous quantity. Rather, it specifies a global property of the quantum evolution. The second measure, called *speed efficiency* $\eta_{SE}(t) \stackrel{\text{def}}{=} \Delta E(t) / \|\mathbf{H}(t)\|_{\text{SP}}$ is an instantaneous quantity.

The key quantity in its definition is the concept of energy or, alternatively, the concept of speed of a quantum evolution in projective Hilbert space given by $v_{\text{H}}(t) \stackrel{\text{def}}{=} \Delta E(t) / \hbar$ (as defined in Ref. [21]). Therefore, when the speed of quantum evolution of the system equals the maximal speed (i.e., $\|\mathbf{H}(t)\|_{\text{SP}} / \hbar$) allotted by the available energetic resources, a maximally speed efficient quantum evolution occurs according to the measure $\eta_{SE}(t)$. When employing $\eta_{SE}(t)$, it only makes sense speaking of energetically un wasteful or energetically wasteful quantum evolutions on a pre-defined and non necessarily geodesic quantum path on the Bloch sphere.

Given the global quantity $\eta_{GE}(t_A, t_B) \stackrel{\text{def}}{=} 2 \arccos [|\langle A|B \rangle|] / \int_{t_A}^{t_B} (2/\hbar) \Delta E(t) dt$ and the local quantity $\eta_{SE}(t) \stackrel{\text{def}}{=} \Delta E(t) / \|\mathbf{H}(t)\|_{\text{SP}}$ with $t_A \leq t \leq t_B$, we wish to define a (global) hybrid measure of efficiency that takes into consideration both deviations from trajectories of shortest length and departures from ideal energetically un wasteful quantum dynamical trajectories on the Bloch sphere. Furthermore, we require this hybrid efficiency measure denoted as η_{HE} to be such that: i) $0 \leq \eta_{\text{HE}} \leq 1$; ii) $\eta_{\text{HE}} = \eta_{\text{HE}}(\bar{\eta}_{\text{GE}}, \bar{\eta}_{\text{SE}})$; iii) $\eta_{\text{HE}} \rightarrow \bar{\eta}_{\text{GE}}$ when $\bar{\eta}_{\text{SE}} \rightarrow 1$; iv) $\eta_{\text{HE}} \rightarrow \bar{\eta}_{\text{SE}}$ when $\bar{\eta}_{\text{GE}} \rightarrow 1$; v) $\eta_{\text{HE}} \leq \min \{\bar{\eta}_{\text{GE}}, \bar{\eta}_{\text{SE}}\}$. The quantities $\bar{\eta}_{\text{GE}}$ and $\bar{\eta}_{\text{SE}}$ are given by

$$\bar{\eta}_{\text{GE}} = \bar{\eta}_{\text{GE}}(t_A, t_B) \stackrel{\text{def}}{=} \frac{1}{t_B - t_A} \int_{t_A}^{t_B} \eta_{\text{GE}}(t) dt, \quad (11)$$

with $\eta_{\text{GE}}(t) \stackrel{\text{def}}{=} 2 \arccos [|\langle A|\psi(t)\rangle|] / \int_{t_A}^t (2/\hbar) \Delta E(t') dt'$, and

$$\bar{\eta}_{\text{SE}} = \bar{\eta}_{\text{SE}}(t_A, t_B) \stackrel{\text{def}}{=} \frac{1}{t_B - t_A} \int_{t_A}^{t_B} \eta_{\text{SE}}(t) dt, \quad (12)$$

respectively. The quantity $\bar{\eta}_{\text{GE}}(t_A, t_B)$ is the average geodesic efficiency of the quantum evolution over the time interval $[t_A, t_B]$. It quantifies the average deviation of the actual evolution from the geodesic evolution. The quantity $\bar{\eta}_{\text{SE}}(t_A, t_B)$, instead, is the average speed efficiency of the quantum evolution over the time interval $[t_A, t_B]$. It describes the average waste of energy resources during the evolution from t_A to t_B . For completeness, we remark that when we define the average speed efficiency $\bar{\eta}_{\text{SE}}$, we are in the presence of a reasonable and global extension of a truly local quantity defined at an instant t (i.e., $\eta_{\text{SE}}(t)$). Unlike $\eta_{\text{SE}}(t)$, $\eta_{\text{GE}}(t)$ is a sort of global quantity since its definition requires the specification of a finite temporal interval $[t_A, t]$. Therefore, when evaluating the average geodesic efficiency $\bar{\eta}_{\text{GE}}$, one needs to take into account the fact that there is an underlying choice of an initial time t_A , with $t_A \leq t' \leq t \leq t_B$ as clear from the definitions of $\eta_{\text{GE}}(t)$ and $\bar{\eta}_{\text{GE}} = \bar{\eta}_{\text{GE}}(t_A, t_B)$. The imposition of the above-mentioned five conditions can be physically explained as follows. To begin, condition i) simply demands that the numerical values assumed by η_{HE} belong to the same range as that specifying the efficiencies η_{GE} and η_{SE} (or, alternatively, $\bar{\eta}_{\text{GE}}$ and $\bar{\eta}_{\text{SE}}$). Condition ii) expresses the reasonable fact that the functional form of η_{HE} must be expressible in terms of $\bar{\eta}_{\text{GE}}$ and $\bar{\eta}_{\text{SE}}$. Furthermore, conditions iii) and iv) require that η_{HE} reduces to $\bar{\eta}_{\text{GE}}$ when there is no average waste of energy or, alternatively, to $\bar{\eta}_{\text{SE}}$ in the absence of any average deviation from a geodesic motion on the Bloch sphere. Finally, since the hybrid efficiency is built so that encodes information about a quantum evolution both in terms of nongeodesicity and energy resources, one expects that it will be generally more demanding (with respect to the efficiencies $\bar{\eta}_{\text{GE}}$ and $\bar{\eta}_{\text{SE}}$, each encoding only one aspect of the quantum evolution) to achieve a high value of η_{HE} . Therefore, we impose $\eta_{\text{HE}} \leq \min \{\bar{\eta}_{\text{GE}}, \bar{\eta}_{\text{SE}}\}$.

Given these five requirements, we propose to consider the following hybrid efficiency measure

$$\eta_{\text{HE}}(t_A, t_B) \stackrel{\text{def}}{=} \bar{\eta}_{\text{GE}}(t_A, t_B) \bar{\eta}_{\text{SE}}(t_A, t_B) \quad (13)$$

By construction, $\eta_{\text{HE}}(t_A, t_B)$ in Eq. (13) satisfies properties i), ii), iii), iv), and v). Note that one may think of considering the arithmetic and the geometric means between $\bar{\eta}_{\text{GE}}$ and $\bar{\eta}_{\text{SE}}$ given by

$$\frac{\bar{\eta}_{\text{GE}} + \bar{\eta}_{\text{SE}}}{2}, \text{ and } \sqrt{\bar{\eta}_{\text{GE}} \bar{\eta}_{\text{SE}}}, \quad (14)$$

respectively. However, both proposals fail to satisfy properties iii), iv), and v). The newly proposed hybrid efficiency measure $\eta_{\text{HE}}(t_A, t_B)$ in Eq. (13) specifies the average deviation of the actual evolution from the geodesic evolution

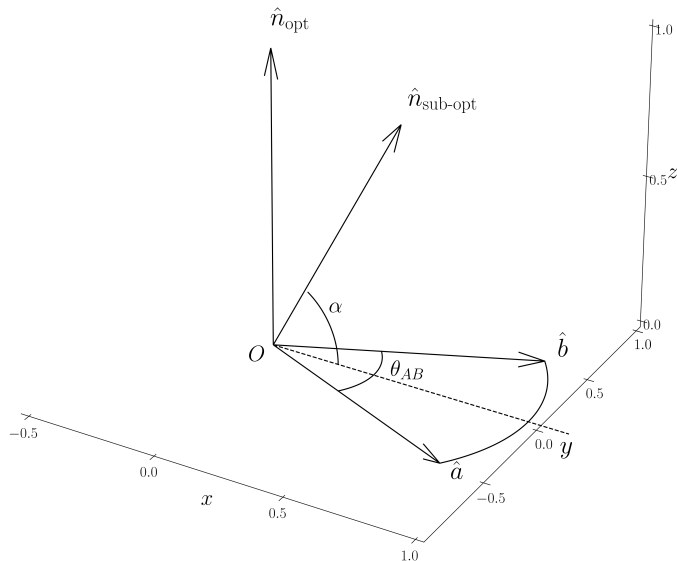


FIG. 1: Schematic depiction of the unit vectors $\hat{n}_{\text{opt}} \stackrel{\text{def}}{=} (\hat{a} \times \hat{b}) / \|\hat{a} \times \hat{b}\|$ and $\hat{n}_{\text{sub-opt}} \stackrel{\text{def}}{=} \cos(\alpha) \left[(\hat{a} + \hat{b}) / \|\hat{a} + \hat{b}\| \right] + \sin(\alpha) \left[(\hat{a} \times \hat{b}) / \|\hat{a} \times \hat{b}\| \right]$ specifying the optimal and sub-optimal rotation axes, respectively. The initial and final Bloch vectors \hat{a} and \hat{b} , respectively, are such that $\hat{a} \cdot \hat{b} = \cos(\theta_{AB})$.

together with the average waste of energy resources over the time interval $[t_A, t_B]$. More explicitly, its interpretation can be explained by considering the following scenarios specified in terms of the original pair of values $(\bar{\eta}_{\text{GE}}, \bar{\eta}_{\text{SE}})$. In the first scenario, assume $(\bar{\eta}_{\text{GE}}, \bar{\eta}_{\text{SE}}) = (1, 1)$. In this case, $\eta_{\text{HE}} = 1$ and we deal with geodesic unwasteful paths. In the second scenario, assume $(\bar{\eta}_{\text{GE}}, \bar{\eta}_{\text{SE}}) = (< 1, 1)$. In this case, $\eta_{\text{HE}} = \bar{\eta}_{\text{GE}} < 1$ and we deal with nongeodesic unwasteful paths. In the third scenario, assume $(\bar{\eta}_{\text{GE}}, \bar{\eta}_{\text{SE}}) = (1, < 1)$. In this case $\eta_{\text{HE}} = \bar{\eta}_{\text{SE}} < 1$, and we deal with geodesic wasteful paths. In the fourth scenario, assume $(\bar{\eta}_{\text{GE}}, \bar{\eta}_{\text{SE}}) = (< 1, < 1)$. In this case, we have three subcases. Before discussing these three subcases, note that $\bar{\eta}_{\text{GE}} = 1 - \langle \Delta s/s \rangle_{\Delta t}$ and $\bar{\eta}_{\text{SE}} = 1 - \langle \Delta \epsilon/\epsilon \rangle_{\Delta t}$, with $\Delta t \stackrel{\text{def}}{=} t_B - t_A$, $\Delta s(t) \stackrel{\text{def}}{=} s(t) - s_0(t)$, $\Delta \epsilon(t) \stackrel{\text{def}}{=} \|\mathbf{H}(t)\|_{\text{SP}} - \Delta E(t)$, and $\epsilon(t) \stackrel{\text{def}}{=} \|\mathbf{H}(t)\|_{\text{SP}}$. Then, in the first subcase, assume $\Delta \epsilon/\epsilon > \Delta s/s$. We deal then with more wasteful than nongeodesic paths. In the second subcase, assume $\Delta \epsilon/\epsilon < \Delta s/s$. We deal then with less wasteful than nongeodesic paths. In the third subcase, finally, assume $\Delta \epsilon/\epsilon = \Delta s/s$. We then deal with as wasteful as nongeodesic paths. In conclusion, by means of $\eta_{\text{HE}}(t_A, t_B)$, we can characterize quantum evolutions in terms of average geodesicity, average energetic waste, and any combination of these two average properties of quantum evolutions over a finite time interval $[t_A, t_B]$. The hybrid measure $\eta_{\text{HE}}(t_A, t_B)$ mimics the behavior of the lowest efficiency measure between $\bar{\eta}_{\text{GE}}$ and $\bar{\eta}_{\text{SE}}$. Specifically, we have the following. In the first scenario, $\eta_{\text{HE}} = \bar{\eta}_{\text{GE}} = \bar{\eta}_{\text{SE}} = 1$ and we are dealing with a geodesic unwasteful evolution. In the second scenario, $\eta_{\text{HE}} = \bar{\eta}_{\text{GE}} < 1$ and we are dealing with a nongeodesic unwasteful evolution. In the third scenario, $\eta_{\text{HE}} = \bar{\eta}_{\text{SE}} < 1$ and we are dealing with a geodesic wasteful evolution. In the first subcase of the fourth case, $\bar{\eta}_{\text{GE}} < 1$ and $\bar{\eta}_{\text{SE}} \ll 1$. Then, $\eta_{\text{HE}} \ll 1$ and we are dealing with more wasteful than nongeodesic evolutions. In the second subcase of the fourth case, since $\bar{\eta}_{\text{GE}} \ll 1$ and $\bar{\eta}_{\text{SE}} < 1$, $\eta_{\text{HE}} \ll 1$ and we are dealing with less wasteful than nongeodesic evolutions. Finally, in the third subcase of the fourth case, we have $\bar{\eta}_{\text{GE}} = \bar{\eta}_{\text{SE}} < 1$. Then $\eta_{\text{HE}} \leq \bar{\eta}_{\text{GE}} = \bar{\eta}_{\text{SE}} < 1$ and we are dealing with evolutions that are as wasteful as nongeodesic. We refer to Table I for a visual summary of all the quantum-mechanical scenarios discussed here.

Having introduced the geodesic, speed, and hybrid efficiencies of quantum evolutions on a Bloch sphere in Eqs. (1), (6), and (13), respectively, we can now discuss sub-optimal quantum evolution scenarios in the next section.

III. DEVIATIONS FROM IDEALITY

In this section, we begin by constructing a one-parameter family of stationary qubit Hamiltonians connecting two states $|A\rangle$ and $|B\rangle$ along nongeodesic paths on the Bloch sphere. We then analyze both non-traceless and traceless nonstationary Hamiltonians yielding energy-wasteful evolutions. In both cases, we quantify aspects of the quantum evolutions in terms of the geodesic and speed efficiencies introduced in the previous section.

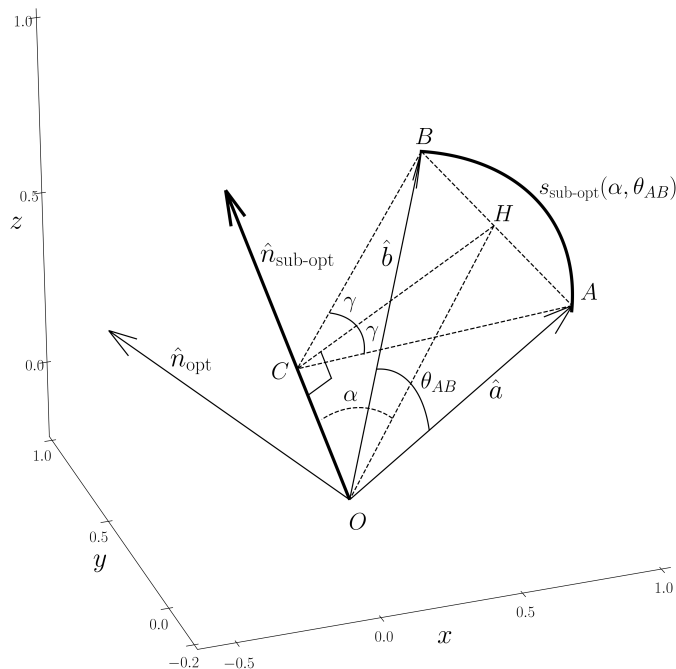


FIG. 2: Schematic depiction of the unit vectors $\hat{n}_{\text{opt}} \stackrel{\text{def}}{=} (\hat{a} \times \hat{b}) / \|\hat{a} \times \hat{b}\|$ and $\hat{n}_{\text{sub-opt}} \stackrel{\text{def}}{=} \cos(\alpha) \left[(\hat{a} + \hat{b}) / \|\hat{a} + \hat{b}\| \right] + \sin(\alpha) \left[(\hat{a} \times \hat{b}) / \|\hat{a} \times \hat{b}\| \right]$ specifying the optimal (thin black) and sub-optimal (thick black) rotation axes, respectively. The initial and final Bloch vectors \hat{a} and \hat{b} , respectively, are such that $\hat{a} \cdot \hat{b} = \cos(\theta_{AB})$. The sub-optimal unitary evolution that evolves \hat{a} into \hat{b} is specified by $\hat{n}_{\text{sub-opt}}$ and a rotation angle $\phi \stackrel{\text{def}}{=} 2\gamma$. Finally, the length of the nongeodesic path connecting these two Bloch vectors via the sub-optimal unitary evolution is given by $s_{\text{sub-opt}}(\alpha, \theta_{AB}) \stackrel{\text{def}}{=} \overline{AC}(\alpha, \theta_{AB}) \phi(\alpha, \theta_{AB})$ (thick black).

A. From geodesic to nongeodesic evolutions

In this subsection, we focus on how to generate sub-optimal unitary operators $U_{\text{sub-opt}}(t)$ such that $U_{\text{sub-opt}}(t_{AB})|A\rangle = |B\rangle$ for arbitrary pure qubit states $|A\rangle$ and $|B\rangle$ with t_{AB} greater than the minimal evolution time that specifies optimal quantum evolutions. In particular, we focus on unitary operators that emerge from stationary traceless Hamiltonians. Essentially, these unitary time propagators act on qubits as rotations around a fixed axis in the Bloch sphere. More specifically, $U_{\text{sub-opt}}(t_{AB}) = e^{-\frac{i}{\hbar} H_{\text{sub-opt}} t_{AB}} = e^{-i \frac{\phi}{2} \hat{n}_{\text{sub-opt}} \cdot \boldsymbol{\sigma}}$. Therefore, we need to find a rotation angle ϕ and a rotation axis $\hat{n}_{\text{sub-opt}}$ with $H_{\text{sub-opt}} \stackrel{\text{def}}{=} E \hat{n}_{\text{sub-opt}} \cdot \boldsymbol{\sigma}$, $(E/\hbar)t_{AB} = \phi/2$, and E expressed in energy units. We point out that, exploiting the correspondence between unit quantum states evolving on the Bloch sphere and unit vectors evolving on a three-dimensional unit sphere, all the results that we obtain in what follows rely on three-dimensional geometry and simple trigonometry. To better explain our geometric reasoning in the following discussions, we refer to Fig. 1 and Fig. 2.

We remark that the derivations contained in this subsection A can be a bit tedious in terms of mathematical details, despite being rather interesting for those intrigued by geometric perspectives on quantum mechanics. The reader, however, could avoid its reading and proceed to subsection B provided that Eqs. (21) and (22) are taken into considerations. Eqs. (21) and (22) are the two main results of subsection A, and are needed to evaluate the geodesic efficiency η_{GE} . They express the travel time $t_{AB}(\alpha)$ and the length of the path $s(\alpha)$, respectively, that correspond to the sub-optimal quantum evolution specified by $H_{\text{sub-opt}}$ in Eq. (17).

Rotation axis $\hat{n}_{\text{sub-opt}}$. Let us begin with the construction of the rotation axis $\hat{n}_{\text{sub-opt}}$. Assume that $\rho_A \stackrel{\text{def}}{=} |A\rangle\langle A| = (\mathbf{1} + \hat{a} \cdot \boldsymbol{\sigma})/2$ and $\rho_B \stackrel{\text{def}}{=} |B\rangle\langle B| = (\mathbf{1} + \hat{b} \cdot \boldsymbol{\sigma})/2$. Since we wish to arrive at \hat{b} from \hat{a} by means of a rotation, the path traced will be a circumference embedded in the unit sphere \hat{a} and \hat{b} belong to. To define this rotation (a member of a larger family of rotations, each one with a specific rotation axis and an angle of rotation), we need to find the axis we have to rotate around and, in addition, the angle needed to transition from \hat{a} to \hat{b} . Any circumference embedded in a sphere can be viewed as the intersection of a plane with the sphere. Since the circumferences we focus on must

contain the tips of \hat{a} and \hat{b} , such planes must contain the tips as well. This implies that the planes we should take into consideration must contain the vector connecting \hat{a} and \hat{b} . Then, the possible axes of rotations will correspond to unit vectors with tail in the origin and, in addition, perpendicular to one of the previously mentioned planes.

In particular, all possible axes of rotation belong to the same plane. The plane can be defined as the two-dimensional vector space spanned by the set of linearly independent vectors $\{\hat{a} \times \hat{b}, \hat{a} + \hat{b}\}$. Note that this is a set of orthogonal non-unit vectors. Moreover, any rotation axis can be defined by a unit vector $\hat{n}_{\text{sub-opt}}$ written as a linear combination of vectors in $\{\hat{a} \times \hat{b}, \hat{a} + \hat{b}\}$. Specifically, $\hat{n}_{\text{sub-opt}}$ can be expressed as

$$\hat{n}_{\text{sub-opt}}(\alpha) \stackrel{\text{def}}{=} \cos(\alpha) \frac{\hat{a} + \hat{b}}{\|\hat{a} + \hat{b}\|} + \sin(\alpha) \frac{\hat{a} \times \hat{b}}{\|\hat{a} \times \hat{b}\|}, \quad (15)$$

with $\alpha \in [0, \pi]$. Assuming $\hat{a} \cdot \hat{b} = \cos(\theta_{AB})$, $\hat{n}_{\text{sub-opt}}(\alpha)$ can be rewritten as

$$\hat{n}_{\text{sub-opt}}(\alpha) = \cos(\alpha) \frac{\hat{a} + \hat{b}}{2 \cos(\frac{\theta_{AB}}{2})} + \sin(\alpha) \frac{\hat{a} \times \hat{b}}{\sin(\theta_{AB})}. \quad (16)$$

Eq. (16) expresses a one-parameter family of unit vectors that determine rotations which bring \hat{a} to \hat{b} . Interestingly, the rotation axis $\hat{n}_{\text{sub-opt}}(\alpha_*)$ that is perpendicular to the plane containing \hat{a} and \hat{b} is denoted as $\hat{n}_{\text{opt}} \stackrel{\text{def}}{=} (\hat{a} \times \hat{b}) / \sin(\theta_{AB})$ for $\alpha_* = \pi/2$. For completeness, we make explicit the fact that the sub-optimal Hermitian Hamiltonian $H_{\text{sub-opt}}$ is given by

$$H_{\text{sub-opt}} = H_{\text{sub-opt}}(\alpha) \stackrel{\text{def}}{=} E \left[\cos(\alpha) \frac{\hat{a} + \hat{b}}{\sqrt{(\hat{a} + \hat{b}) \cdot (\hat{a} + \hat{b})}} + \sin(\alpha) \frac{\hat{a} \times \hat{b}}{\sqrt{(\hat{a} \times \hat{b}) \cdot (\hat{a} \times \hat{b})}} \right] \cdot \sigma, \quad (17)$$

and, clearly, the unitary time propagator is $U_{\text{sub-opt}}(t) = \exp(-\frac{i}{\hbar} H_{\text{sub-opt}} t)$.

Rotation angle ϕ . Let us recast the rotation angle as $\phi = 2\gamma$. From the drawing in Fig. 1, consider the rectangular triangle AHC (where the angle $\angle AHC$ is equal to 90°). Then, from $\overline{CH} = \overline{AC} \cos(\gamma)$, we get $\gamma = \arccos(\overline{CH}/\overline{AC})$. The lengths of the sides \overline{CH} and \overline{AC} can be expressed in terms of the angles α and θ_{AB} . From Fig. 1, $\overline{CH} = \overline{OH} \sin(\alpha)$, with $\overline{OH} = \left\| (\hat{a} + \hat{b})/2 \right\| = \cos(\theta_{AB}/2)$. This is a consequence of the fact that the triangle OCH is rectangular, with the angle $\angle OCH$ equal to 90° . Therefore, $\overline{CH} = \sin(\alpha) \cos(\theta_{AB}/2)$. For clarity, observe that $\overline{OA} = \overline{OB} = 1$. Furthermore, since \overline{AC} is the perpendicular component of \hat{a} with respect to $\hat{n}_{\text{sub-opt}}$, it can be expressed as the modulus of the cross product between \hat{a} and $\hat{n}_{\text{sub-opt}}$. Specifically, we have $\overline{AC} = \|\hat{n}_{\text{sub-opt}} \times \hat{a}\| = \sqrt{(\hat{n}_{\text{sub-opt}} \times \hat{a}) \cdot (\hat{n}_{\text{sub-opt}} \times \hat{a})}$ with $\hat{a} = (\hat{a} \cdot \hat{n}_{\text{sub-opt}}) \hat{n}_{\text{sub-opt}} + [\hat{a} - (\hat{a} \cdot \hat{n}_{\text{sub-opt}}) \hat{n}_{\text{sub-opt}}] = \hat{a}_{\parallel} + \hat{a}_{\perp}$, $\hat{n}_{\text{sub-opt}} \times \hat{a}_{\parallel} = 0$. Therefore, $\overline{AC} = \|\hat{n}_{\text{sub-opt}} \times \hat{a}_{\perp}\| = \|\hat{a}_{\perp}\|$. After some algebra and use of Eq. (16), we get

$$\overline{AC} = \overline{AC}(\alpha) \stackrel{\text{def}}{=} \sqrt{\frac{\cos^2(\alpha)}{4 \cos^2(\frac{\theta_{AB}}{2})} \sin^2(\theta_{AB}) + \sin^2(\alpha)}. \quad (18)$$

Recalling that $\sin^2(\alpha) = 1 - \cos^2(\alpha)$ and $\sin^2(\theta_{AB}) = 4 \sin^2(\theta_{AB}/2) \cos^2(\theta_{AB}/2)$, \overline{AC} in Eq. (18) can be rewritten as

$$\overline{AC}(\alpha) = \sqrt{1 - \cos^2(\alpha) \cos^2\left(\frac{\theta_{AB}}{2}\right)}. \quad (19)$$

We emphasize that while Eq. (18) is derived using pure geometric arguments and, in addition, the transition from Eq. (18) to Eq. (19) relies on simple trigonometric manipulations, the more succinct and geometric formula in Eq. (19) can be shown to yield $\overline{AC}(\alpha) = \sqrt{1 - \cos^2(\alpha) \cos^2(\theta_{AB}/2)} = \Delta E(\alpha)/E$ thanks to quantum mechanics rules needed for the calculation of the energy uncertainty of the system $\Delta E(\alpha)$. For more details, we refer to Appendix A. Finally, having expressed \overline{CH} and \overline{AC} in terms of α and θ_{AB} , the rotation angle $\phi = 2\gamma = 2 \arccos(\overline{CH}/\overline{AC})$ is given by

$$\phi = \phi(\alpha) \stackrel{\text{def}}{=} 2 \arccos\left(\frac{\sin(\alpha) \cos(\frac{\theta_{AB}}{2})}{\sqrt{1 - \cos^2(\alpha) \cos^2(\frac{\theta_{AB}}{2})}}\right) = 2 \arccos\left(\tan(\alpha) \frac{\|\hat{a}_{\parallel}, \hat{n}_{\text{sub-opt}}\|}{\sqrt{1 - \|\hat{a}_{\parallel}, \hat{n}_{\text{sub-opt}}\|^2}}\right). \quad (20)$$

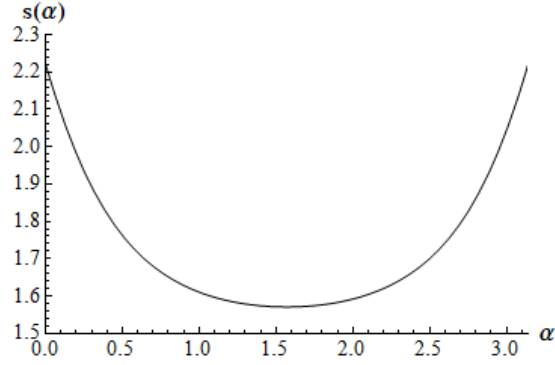


FIG. 3: Plot of the length $s = s(\alpha) \stackrel{\text{def}}{=} s_{\text{sub-opt}}(\alpha, \theta_{AB})$ of the path generated by the Hamiltonian $H_{\text{sub-opt}}(\alpha)$ that connects two states $|A\rangle$ and $|B\rangle$ with corresponding Bloch vectors \hat{a} and \hat{b} , respectively, with $\hat{a} \cdot \hat{b} = \cos(\theta_{AB})$. We set $\theta_{AB} = \pi/2$ and visualize $s(\alpha)$ versus α , with $0 \leq \alpha \leq \pi$. Note that the minimum s is reached at $\alpha = \pi/2 \simeq 1.57$ (i.e., when $H_{\text{sub-opt}}(\alpha)$ becomes H_{opt}), with s equal to $\pi/2$ (i.e., one-half of the shortest length π between two orthogonal quantum states on the Bloch sphere).

In the last equality of Eq. (20), we expressed the rotation angle solely in terms of α and the magnitude of \hat{a}_{\parallel} , $\hat{n}_{\text{sub-opt}} \stackrel{\text{def}}{=} (\hat{a} \cdot \hat{n}_{\text{sub-opt}}) \hat{n}_{\text{sub-opt}}$. With the derivations of $\hat{n}_{\text{sub-opt}}(\alpha)$ in Eq. (16) and $\phi(\alpha)$ in Eq. (20), we can finally express in an explicit manner $U_{\text{sub-opt}}(t_{AB}) = e^{-i \frac{\sigma}{2} \hat{n}_{\text{sub-opt}} \cdot \vec{\sigma}}$ with $t_{AB} = t_{AB}(\alpha) \stackrel{\text{def}}{=} [\hbar/(2E)] \phi(\alpha)$.

Travel time and length of the path. The travel time is simply given by $t_{AB} = t_{AB}(\alpha) \stackrel{\text{def}}{=} [\hbar/(2E)] \phi(\alpha)$. Its explicit expression is

$$t_{AB}(\alpha) = \frac{\hbar}{E} \arccos \left(\frac{\sin(\alpha) \cos\left(\frac{\theta_{AB}}{2}\right)}{\sqrt{1 - \cos^2(\alpha) \cos^2\left(\frac{\theta_{AB}}{2}\right)}} \right). \quad (21)$$

Interestingly, we observe that the minimum of $t_{AB}(\alpha)$ in Eq. (21) is achieved at $\alpha = \pi/2$, for any θ_{AB} . Since $\alpha = \pi/2$ implies $\hat{n}_{\text{sub-opt}} = \hat{n}_{\text{opt}}$, the path is a geodesic since \hat{a} rotates perpendicularly about \hat{n}_{opt} . Indeed, as α approaches $\pi/2$, $t_{AB}(\alpha)$ approaches the optimal (i.e., shortest) travel time given by $t_{AB}^{\text{opt}} = [\hbar/(2E)] \theta_{AB}$. Moreover, the length s of the arc traced on the sphere during the motion is given by $s = s(\alpha) \stackrel{\text{def}}{=} \overline{AC}(\alpha) \phi(\alpha)$. Explicitly, we have

$$s(\alpha) \stackrel{\text{def}}{=} 2 \arccos \left(\frac{\sin(\alpha) \cos\left(\frac{\theta_{AB}}{2}\right)}{\sqrt{1 - \cos^2(\alpha) \cos^2\left(\frac{\theta_{AB}}{2}\right)}} \right) \cdot \sqrt{1 - \cos^2(\alpha) \cos^2\left(\frac{\theta_{AB}}{2}\right)}. \quad (22)$$

As a simple cross check of the correctness of the expression for $s(\alpha)$ in Eq. (22), we consider the case of two antipodal vectors \hat{a} and \hat{b} . In this case, we have $\theta_{AB} = \pi$ and we expect the length of the arc $s(\alpha)$ to be independent from the particular axis of rotation and equal to π . This is justified by the fact that any rotation transporting the initial state to the final state will trace on the unit sphere an arc that corresponds to a semi-circumference of unit radius. Indeed, it happens that $s(\alpha) \rightarrow \pi$ as $\theta_{AB} \rightarrow \pi$, for any choice of α . Moreover, for $\alpha = \pi/2$, we note that $s(\alpha)$ in Eq. (22) reduces to its optimal (i.e., shortest) limiting value $s_{\text{opt}} = \theta_{AB}$. In our opinion, it is remarkable that $s(\alpha)$ in Eq. (22) was obtained by means of simple geometric arguments. Even more remarkable, is that we can explicitly show that it coincides with the usual length of the path defined by Anandan and Aharonov as

$$s \stackrel{\text{def}}{=} \int_0^{t_{AB}} 2 \frac{\Delta E(t)}{\hbar} dt = 2 \frac{\Delta E}{\hbar} t_{AB}, \quad (23)$$

with ΔE being the energy uncertainty defined as $\Delta E \stackrel{\text{def}}{=} \left[\langle A | H_{\text{sub-opt}}^2 | A \rangle - \langle A | H_{\text{sub-opt}} | A \rangle^2 \right]^{1/2}$. Interestingly, we can verify that $\Delta E = \Delta E(\alpha) \stackrel{\text{def}}{=} E \sqrt{1 - \cos^2(\alpha) \cos^2\left(\frac{\theta_{AB}}{2}\right)} = E \cdot \overline{AC}(\alpha)$. For details on the calculation of $\Delta E(\alpha)$ with ordinary (i.e., non-geometric) quantum mechanics rules, we refer to Appendix A. Thus, recalling the expression of $t_{AB}(\alpha)$ in Eq. (21), it turns out that the “quantum” s in Eq. (23) coincides with the “geometric” s in Eq. (22).

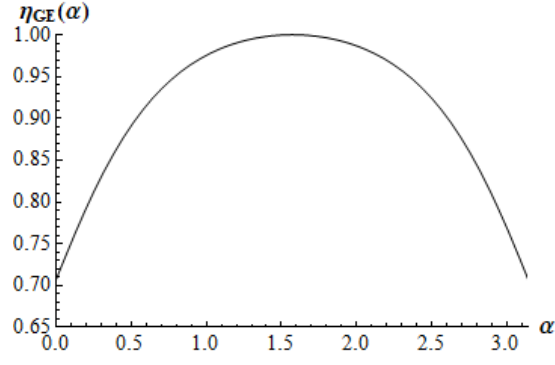


FIG. 4: Plot of the geodesic efficiency $\eta_{\text{GE}}(\alpha)$ versus α , with $0 \leq \alpha \leq \pi$. The sub-optimal quantum evolution specified by the stationary Hamiltonian $H_{\text{sub-opt}}(\alpha)$ is assumed to connect $|A\rangle$ with $|B\rangle$ with corresponding Bloch vectors \hat{a} and \hat{b} , respectively, where $\hat{a} \cdot \hat{b} = \cos(\theta_{AB})$. In the plot, we set $\theta_{AB} = \pi/2$. Observe that the maximum geodesic efficiency value equal to one is obtained for $\alpha = \pi/2 \simeq 1.57$, when $H_{\text{sub-opt}}(\alpha)$ reduces to the optimal Hamiltonian H_{opt} .

Using Eqs. (19), (22) and (23), $s_{\text{sub-opt}}$ can be conveniently rewritten as

$$s_{\text{sub-opt}} = s_{\text{sub-opt}}(\alpha) \stackrel{\text{def}}{=} 2\sqrt{1 - \cos^2(\alpha) \cos^2\left(\frac{\theta_{AB}}{2}\right)} \arccos\left[\sin(\alpha) \frac{\cos\left(\frac{\theta_{AB}}{2}\right)}{\sqrt{1 - \cos^2(\alpha) \cos^2\left(\frac{\theta_{AB}}{2}\right)}}\right]. \quad (24)$$

In Fig. 3, we show the behavior of $s(\alpha)$ as a function of the parameter α . Finally, we plot in Fig. 4 the geodesic efficiency $\eta_{\text{GE}}(\alpha) \stackrel{\text{def}}{=} \theta_{AB}/s_{\text{sub-opt}}(\alpha)$ versus α . We note that for $\theta_{AB} = \pi/2$ and α very close to $\pi/2$, the approximate behavior of $\eta_{\text{GE}}(\alpha)$ is given by

$$\eta_{\text{GE}}(\alpha) = 1 - \frac{4 - \pi}{4\pi} \left(\alpha - \frac{\pi}{2}\right)^2 + O(\alpha^3). \quad (25)$$

We are now ready to study both non-traceless and traceless time-varying qubit Hamiltonians that lead to energy-wasteful quantum evolutions.

B. From energy-resourceful to energy-wasteful evolutions

Focusing on two-level quantum systems, we recall that in Ref. [21] a unit speed efficiency Hamiltonian evolution with $\eta_{\text{SE}} \stackrel{\text{def}}{=} \Delta H_\rho / \|H\|_{\text{SP}} = 1$ is specified by $H_{\text{opt}}(t) \stackrel{\text{def}}{=} i|\partial_t m(t)\rangle \langle m(t)| - i|m(t)\rangle \langle \partial_t m(t)|$ as in Eq. (10), where $i\partial_t |m(t)\rangle = H_{\text{opt}}(t) |m(t)\rangle$ and $H_{\text{opt}}(t)$ is a traceless Hermitian operator. Setting $|m\rangle = |m(t)\rangle \stackrel{\text{def}}{=}} c_0(t)|0\rangle + c_1(t)|1\rangle$ with $|c_0(t)|^2 + |c_1(t)|^2 = 1$, a straightforward calculation yields $\Delta H_\rho^2 = \langle m | H_{\text{opt}}^2 | m \rangle - \langle m | H_{\text{opt}} | m \rangle^2 = \langle \dot{m} | \dot{m} \rangle - 0 = |\dot{c}_0|^2 + |\dot{c}_1|^2$ and $\|H\|_{\text{SP}}^2 = |\dot{c}_0|^2 + |\dot{c}_1|^2$. Clearly, the dot denotes here differentiation with respect to the time variable t . Therefore, the speed efficiency becomes

$$\eta_{\text{SE}}^{\text{H}_{\text{opt}}}(t) = \frac{\sqrt{|\dot{c}_0|^2 + |\dot{c}_1|^2}}{\sqrt{|\dot{c}_0|^2 + |\dot{c}_1|^2}} = 1 \quad (26)$$

for any t and, in addition, $H_{\text{opt}}(t)$ evolves the state $|m(t)\rangle$ with maximal speed and no waste of energy resources. A class of suboptimal Hamiltonian evolutions that generates the same path in projective Hilbert space can be specified by the Hamiltonian given by [21]

$$H_{\text{sub-opt}}^{(\text{trace} \neq 0)}(t) \stackrel{\text{def}}{=} H_{\text{opt}}(t) + \dot{\phi} |m\rangle \langle m|, \quad (27)$$

with the phase $\phi = \phi(t) \in \mathbb{R}$ and $i\partial_t (e^{-i\phi(t)} |m(t)\rangle) = H_{\text{sub-opt}}^{(\text{trace} \neq 0)}(e^{-i\phi(t)} |m(t)\rangle)$. Setting $|m\rangle = |m(t)\rangle \stackrel{\text{def}}{=} c_0(t)|0\rangle + c_1(t)|1\rangle$ with $|c_0(t)|^2 + |c_1(t)|^2 = 1$ and $H \stackrel{\text{def}}{=} H_{\text{sub-opt}}^{(\text{trace} \neq 0)}$, a simple computation leads to $\Delta H_\rho^2 = \langle m | H^2 | m \rangle -$

$\langle m | \mathbf{H} | m \rangle^2 = (\langle \dot{m} | \dot{m} \rangle + \dot{\phi}^2) - \dot{\phi}^2 = |\dot{c}_0|^2 + |\dot{c}_1|^2$ and $\|\mathbf{H}\|_{\text{SP}}^2 = \dot{\phi}^2/2 + |\dot{c}_0|^2 + |\dot{c}_1|^2 + (|\dot{\phi}|/2)\sqrt{\dot{\phi}^2 + 4(|\dot{c}_0|^2 + |\dot{c}_1|^2)}$. Therefore, the speed efficiency reduces to

$$\eta_{\text{SE}}^{\text{H}_{\text{sub-opt}}^{(\text{trace} \neq 0)}}(t) = \frac{\sqrt{|\dot{c}_0|^2 + |\dot{c}_1|^2}}{\sqrt{\frac{\dot{\phi}^2}{2} + (|\dot{c}_0|^2 + |\dot{c}_1|^2) + \frac{|\dot{\phi}|}{2}\sqrt{\dot{\phi}^2 + 4(|\dot{c}_0|^2 + |\dot{c}_1|^2)}}} \quad (28)$$

with $0 \leq \eta_{\text{SE}}^{\text{H}_{\text{sub-opt}}^{(\text{trace} \neq 0)}}(t) \leq 1$. From Eqs. (26) and (28), the available energy resources increase thanks to phase changes. Indeed, the size of $\text{H}_{\text{sub-opt}}^{(\text{trace} \neq 0)}$ is greater than the size of H_{opt} , $\|\text{H}_{\text{sub-opt}}^{(\text{trace} \neq 0)}\|_{\text{SP}} \geq \|\text{H}_{\text{opt}}\|_{\text{SP}}$. Unfortunately, this increase in resources is wasted since the speeds of quantum evolutions along the paths $t \mapsto |m(t)\rangle$ and $t \mapsto e^{-i\phi(t)}|m(t)\rangle$ corresponding to H_{opt} and $\text{H}_{\text{sub-opt}}^{(\text{trace} \neq 0)}$, respectively, remain the same (i.e., $v_{\text{H}_{\text{opt}}} = v_{\text{H}_{\text{sub-opt}}^{(\text{trace} \neq 0)}}$ since $(\Delta \text{H}_{\text{opt}})_\rho = (\Delta \text{H}_{\text{sub-opt}}^{(\text{trace} \neq 0)})_\rho$ with $\rho = \rho(t) \stackrel{\text{def}}{=} |m(t)\rangle \langle m(t)|$). In this sense, phase changes have a negative energetic effect and should be avoided. Interestingly, in the event that phase changes do occur, traceless sub-optimal Hamiltonians $\text{H}_{\text{sub-opt}}^{(\text{trace}=0)}$ defined as

$$\text{H}_{\text{sub-opt}}^{(\text{trace}=0)}(t) \stackrel{\text{def}}{=} \text{H}_{\text{sub-opt}}^{(\text{trace} \neq 0)}(t) - \frac{1}{2} \text{tr}(\dot{\phi} |m\rangle \langle m|) \mathbf{1} = \text{H}_{\text{sub-opt}}^{(\text{trace} \neq 0)}(t) - \frac{1}{2} \dot{\phi} \mathbf{1}, \quad (29)$$

with $\text{H}_{\text{sub-opt}}^{(\text{trace}=0)}(e^{-i\frac{\phi(t)}{2}}|m\rangle) = i\partial_t(e^{-i\frac{\phi(t)}{2}}|m\rangle)$, yield paths $t \mapsto e^{-i\frac{\phi(t)}{2}}|m(t)\rangle$ on the Bloch sphere that are less energy wasteful than those of the nonzero trace sub-optimal Hamiltonians $\text{H}_{\text{sub-opt}}^{(\text{trace} \neq 0)}(t)$ in Eq. (27). For clarity, observe that $\text{tr}(\dot{\phi} |m\rangle \langle m|)$ in Eq. (29) is equal to $\text{tr}(\text{H}_{\text{sub-opt}}^{(\text{trace} \neq 0)})$ since $\text{tr}(\text{H}_{\text{opt}}) = 0$. Traces can be evaluated, for instance, with respect to the orthonormal basis $\{|m\rangle, |\dot{m}\rangle/\sqrt{\langle \dot{m} | \dot{m} \rangle}\}$. Then, putting $|m\rangle = |m(t)\rangle \stackrel{\text{def}}{=}} c_0(t)|0\rangle + c_1(t)|1\rangle$, with $|c_0(t)|^2 + |c_1(t)|^2 = 1$ and $\text{H}_{\text{sub-opt}} \stackrel{\text{def}}{=} \text{H}_{\text{sub-opt}}^{(\text{trace}=0)}$, an easy calculation implies that $\Delta \text{H}_\rho^2 = \langle m | \text{H}^2 | m \rangle - \langle m | \mathbf{H} | m \rangle^2 = (\langle \dot{m} | \dot{m} \rangle + \dot{\phi}^2/4) - \dot{\phi}^2/4 = |\dot{c}_0|^2 + |\dot{c}_1|^2$ and $\|\mathbf{H}\|_{\text{SP}}^2 = \dot{\phi}^2/4 + |\dot{c}_0|^2 + |\dot{c}_1|^2$. Therefore, the speed efficiency reduces to

$$\eta_{\text{SE}}^{\text{H}_{\text{sub-opt}}^{(\text{trace}=0)}}(t) = \frac{\sqrt{|\dot{c}_0|^2 + |\dot{c}_1|^2}}{\sqrt{\frac{\dot{\phi}^2}{4} + (|\dot{c}_0|^2 + |\dot{c}_1|^2)}}, \quad (30)$$

with $0 \leq \eta_{\text{SE}}^{\text{H}_{\text{sub-opt}}^{(\text{trace} \neq 0)}}(t) \leq \eta_{\text{SE}}^{\text{H}_{\text{sub-opt}}^{(\text{trace}=0)}}(t) \leq \eta_{\text{SE}}^{\text{H}_{\text{opt}}}(t) = 1$ for any t . It is worthwhile pointing out that when we set $|\dot{c}_0|^2 + |\dot{c}_1|^2 = \mathcal{A}^2$ and assume $\dot{\phi}^2/(4\mathcal{A}^2) \ll 1$, the approximate behavior of $\eta_{\text{SE}}^{\text{H}_{\text{sub-opt}}^{(\text{trace}=0)}}$ in Eq. (30) as a function of $\dot{\phi}$ is given by

$$\eta_{\text{SE}}^{\text{H}_{\text{sub-opt}}^{(\text{trace}=0)}}(\dot{\phi}) = 1 - \frac{1}{8\mathcal{A}^2} \dot{\phi}^2 + O(\dot{\phi}^3). \quad (31)$$

Moreover, from Eqs. (28) and (30), we note that although the speed of quantum evolutions generated by $\text{H}_{\text{sub-opt}}^{(\text{trace} \neq 0)}$ and $\text{H}_{\text{sub-opt}}^{(\text{trace}=0)}$ are identical, the size of $\text{H}_{\text{sub-opt}}^{(\text{trace}=0)}$ is smaller than the size of $\text{H}_{\text{sub-opt}}^{(\text{trace} \neq 0)}$. Therefore, $\text{H}_{\text{sub-opt}}^{(\text{trace}=0)}$ yields paths on the Bloch sphere that are less energy wasteful than those created by $\text{H}_{\text{sub-opt}}^{(\text{trace} \neq 0)}$. To be clear, although the paths are actually the same in projective Hilbert space in both scenarios, in the more wasteful scenario a greater amount of energy is wasted in the generation of global phases of the evolving quantum state since it is not converted in (useful) speed of the quantum evolution. In Fig. 5, we plot $\eta_{\text{SE}}(\dot{\phi})$ in Eq. (30) versus $\dot{\phi}$ for a suitable choice of $|m(t)\rangle$. Then, assuming to consider the same $|m(t)\rangle$, we plot $\eta_{\text{SE}}(t)$ in Eq. (30) versus t for logarithmic, linear, and exponential temporal growths of the phase $\phi(t)$ in Fig. 6.

For a final remark, let $\rho = \rho(t) \stackrel{\text{def}}{=} |m(t)\rangle \langle m(t)| = [\mathbf{1} + \hat{a}(t) \cdot \boldsymbol{\sigma}]/2$. Then, it is worthwhile pointing out that if we recast the Hamiltonians $\text{H}(t) = \text{H}_{\text{opt}}(t)$ along with those in Eqs. (27) and (29) as $\text{H}(t) = \mathbf{h}_{\text{opt}}(t) \cdot \boldsymbol{\sigma}$, $\text{H}_{\text{sub-opt}}^{(\text{trace} \neq 0)}(t) = h_0(t) \mathbf{1} + \mathbf{h}_{\text{sub-opt}}^{(\text{trace} \neq 0)}(t) \cdot \boldsymbol{\sigma}$, and $\text{H}_{\text{sub-opt}}^{(\text{trace}=0)}(t) = \mathbf{h}_{\text{sub-opt}}^{(\text{trace}=0)}(t) \cdot \boldsymbol{\sigma}$, respectively, we get $\hat{a}(t) \cdot \mathbf{h}_{\text{opt}}(t) = 0$, $h_0(t) + \hat{a}(t) \cdot \mathbf{h}_{\text{sub-opt}}^{(\text{trace} \neq 0)}(t) = \dot{\phi}(t) \neq 0$, and $\hat{a}(t) \cdot \mathbf{h}_{\text{sub-opt}}^{(\text{trace}=0)}(t) = \dot{\phi}(t) - (1/2)\text{tr}(\dot{\phi} |m\rangle \langle m|) \neq 0$. Then, since $\eta_{\text{SE}} = \eta_{\text{SE}}(t) \stackrel{\text{def}}{=}$

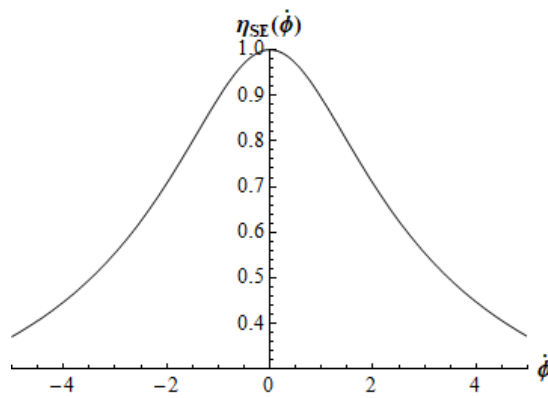


FIG. 5: Plot of the speed efficiency $\eta_{\text{SE}}(\dot{\phi})$ in Eq. (30) versus the rate of change $\dot{\phi}$ of the phase ϕ , with $-5 \leq \dot{\phi} \leq 5$ for $H_{\text{sub-opt}}^{(\text{trace}=0)}$. The sub-optimal quantum evolution is specified by a nonstationary traceless Hamiltonian $H_{\text{sub-opt}}^{(\text{trace}=0)}$ described by a state $|m(t)\rangle \stackrel{\text{def}}{=} \cos(\omega_0 t)|0\rangle + \sin(\omega_0 t)|1\rangle$ and an arbitrary phase $\phi = \phi(t)$. For simplicity, we set $\omega_0 = 1$ in the plot. Physical units are specified by the choice of setting $\hbar = 1$.

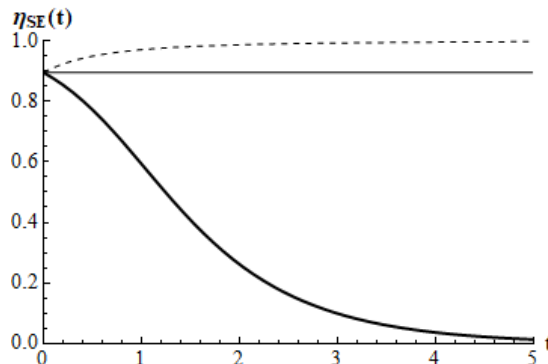


FIG. 6: Plots of the speed efficiency $\eta_{\text{SE}}(t)$ in Eq. (30) versus time t , with $0 \leq t \leq 5$, for three scenarios specified by nonstationary traceless Hamiltonians $H_{\text{sub-opt}}^{(\text{trace}=0)}$ described by the state $|m(t)\rangle \stackrel{\text{def}}{=} \cos(\omega_0 t)|0\rangle + \sin(\omega_0 t)|1\rangle$ and phases $\phi(t) \stackrel{\text{def}}{=} \phi_0 \ln \left[1 + \left(\dot{\phi}_0 / \phi_0 \right) t \right]$ (dashed line), $\phi(t) \stackrel{\text{def}}{=} \phi_0 + \dot{\phi}_0 t$ (thin solid line), and $\phi(t) \stackrel{\text{def}}{=} \phi_0 + (e^{\dot{\phi}_0 t} - 1)$ (thick solid line). Note that $\phi_0 \stackrel{\text{def}}{=} \phi(0)$ and $\dot{\phi}_0 \stackrel{\text{def}}{=} \dot{\phi}(0)$ in all three cases. For simplicity, we set in all three plots $\omega_0 = 1$, $\phi_0 = 1$, and $\dot{\phi}_0 = 1$. Physical units are determined so that $\hbar = 1$.

$\sqrt{\mathbf{h}^2 - (\hat{\mathbf{a}} \cdot \mathbf{h})^2} / (|h_0| + \sqrt{\mathbf{h}^2})$, traceless Hamiltonian evolutions are not energy-wasteful only when $\hat{\mathbf{a}} \cdot \mathbf{h} = 0$. Instead, nonzero trace Hamiltonian evolutions are always energy-wasteful. Summarizing, we conclude that there is no waste of energy resources only for a quantum evolution governed by a traceless Hamiltonian specified by a magnetic field vector $\mathbf{h}_{\text{opt}}(t)$ that is constantly orthogonal to the Bloch vector $\hat{\mathbf{a}}(t)$. This could be interpreted as “instantaneous geodesic motion”, since at every instant of time $\hat{\mathbf{a}}(t)$ instantaneously rotates perpendicularly to $\mathbf{h}(t)$.

We are now ready to discuss some illustrative examples where we characterize quantum evolutions in terms of geodesic, speed, and hybrid efficiency measures.

IV. ILLUSTRATIVE EXAMPLES

In this section, we exploit the formalism presented in the previous section to study four illustrative examples. In particular, we display with these four examples the full spectrum of possible quantum evolutions: Geodesic unwasteful, geodesic wasteful, nongeodesic wasteful and, finally, nongeodesic unwasteful evolutions. For each scenario, we characterize the average properties of the quantum motion by means of the newly proposed hybrid efficiency measure η_{SE} in Eq. (13).

A. First example: $(\eta_{\text{GE}}, \eta_{\text{SE}}) = (1, 1)$

To begin, we note that the stationary Hamiltonian $H_{\text{opt}} = H_{\text{sub-opt}}(\alpha)$ with $\alpha = \pi/2$ and $H_{\text{sub-opt}}(\alpha)$ in Eq. (17) yields quantum evolutions with $(\eta_{\text{GE}}, \eta_{\text{SE}}) = (1, 1)$. However, we wish to present a time-varying setting here. In this first example, we discuss a case in which the quantum evolution is specified by a nonstationary Hamiltonian that yields an energy resourceful geodesic path on the Bloch sphere. In other words, a path along which both the geodesic efficiency η_{GE} and the speed efficiency η_{SE} are equal to one. We construct the Hamiltonian within the framework proposed by Uzdin and collaborators in Ref. [21]. Consider the following unit state vector $|m(t)\rangle$ defined as,

$$|m(t)\rangle \stackrel{\text{def}}{=} \cos\left(\frac{\theta(t)}{2}\right)|0\rangle + e^{i\varphi_0} \sin\left(\frac{\theta(t)}{2}\right)|1\rangle, \quad (32)$$

with $\varphi_0 \neq 0$. Eq. (32) represents a geodesic orbit since the path on the Bloch sphere is a curve of constant longitude $\varphi = \varphi_0$ circumnavigating the poles, with a speed that varies with $\dot{\theta}$. From Eq. (32), we note that $\langle m(t)|m(t)\rangle = 1$ and $\langle \dot{m}(t)|m(t)\rangle = 0$. The unit Bloch vector $\hat{a}(t)$ that corresponds to the pure state $|m(t)\rangle$ is given by $\hat{a}(t) \stackrel{\text{def}}{=} (\sin(\theta)\cos(\varphi_0), \sin(\theta)\sin(\varphi_0), \cos(\theta))$, with $\rho(t) \stackrel{\text{def}}{=} |m(t)\rangle\langle m(t)| = [\mathbf{1} + \hat{a}(t) \cdot \boldsymbol{\sigma}]/2$. Given $|m(t)\rangle$ in Eq. (32), we get that the matrix representation of the traceless Hamiltonian $H(t) \stackrel{\text{def}}{=} i(|\dot{m}\rangle\langle m| - |m\rangle\langle \dot{m}|)$ with respect to the computational basis $\{|0\rangle, |1\rangle\}$ is given by

$$H(t) = \begin{pmatrix} 0 & -ie^{-i\varphi_0}\frac{\dot{\theta}}{2} \\ ie^{i\varphi_0}\frac{\dot{\theta}}{2} & 0 \end{pmatrix}, \quad (33)$$

where $H(t)|m(t)\rangle = i\partial_t|m(t)\rangle$. Then, setting $H(t) = \mathbf{h}(t) \cdot \boldsymbol{\sigma}$, we get

$$\mathbf{h}(t) \stackrel{\text{def}}{=} \left(-\frac{1}{2}\dot{\theta}\sin(\varphi_0), \frac{1}{2}\dot{\theta}\cos(\varphi_0), 0\right). \quad (34)$$

Note that using $\hat{a}(t) \stackrel{\text{def}}{=} (\sin(\theta)\cos(\varphi_0), \sin(\theta)\sin(\varphi_0), \cos(\theta))$ and $\mathbf{h}(t)$ in Eq. (34), we correctly get that $\partial_t\hat{a}(t) = 2\mathbf{h}(t) \times \hat{a}(t)$, $\forall t$. From Eq. (34), we have $\mathbf{h}(t) = h(t)\hat{h}(t)$ with a time-varying intensity $h(t) = \sqrt{\dot{\theta}^2/4}$ and a time-constant direction $\hat{h}(t) = -\sin(\varphi_0)\hat{x} + \cos(\varphi_0)\hat{y}$ so that $\partial_t\hat{h}(t) = \mathbf{0}$. Furthermore, $\mathbf{h}(t)$ is constantly perpendicular to the Bloch vector given that $\hat{a}(t) \cdot \mathbf{h}(t) = 0$ for any t . From $\hat{a} \cdot \mathbf{h} = 0$, we get $\partial_t\hat{a} \cdot \mathbf{h} + \hat{a} \cdot \dot{\mathbf{h}} = 0$. However, since $\partial_t\hat{a} = 2\mathbf{h} \times \hat{a}$ implies that $\partial_t\hat{a} \cdot \mathbf{h} = 0$, we get that $\hat{a} \cdot \dot{\mathbf{h}} = 0$ when $\hat{a} \cdot \mathbf{h} = 0$. Then, since \mathbf{h} does not change in direction, \mathbf{h} and $\dot{\mathbf{h}}$ are collinear. Given these geometric relations, it is worth pointing out that the time-dependent curvature coefficient $\kappa_{\text{AC}}^2(\hat{a}, \mathbf{h})$ given by [32, 33]

$$\kappa_{\text{AC}}^2(\mathbf{a}, \mathbf{h}) \stackrel{\text{def}}{=} 4\frac{(\mathbf{a} \cdot \mathbf{h})^2}{\mathbf{h}^2 - (\mathbf{a} \cdot \mathbf{h})^2} + \frac{\left[\mathbf{h}^2\dot{\mathbf{h}}^2 - (\mathbf{h} \cdot \dot{\mathbf{h}})^2\right] - \left[(\mathbf{a} \cdot \dot{\mathbf{h}})\mathbf{h} - (\mathbf{a} \cdot \mathbf{h})\dot{\mathbf{h}}\right]^2}{\left[\mathbf{h}^2 - (\mathbf{a} \cdot \mathbf{h})^2\right]^3} + 4\frac{(\mathbf{a} \cdot \mathbf{h})\left[\mathbf{a} \cdot (\mathbf{h} \times \dot{\mathbf{h}})\right]}{\left[\mathbf{h}^2 - (\mathbf{a} \cdot \mathbf{h})^2\right]^2}, \quad (35)$$

with $\hat{a} = \mathbf{a}$ is identically zero and the evolution is geodesic. The interested reader can find technical details leading to Eq. (35) in Appendix B. In Eq. (35), ‘‘AC’’ means Alsing and Cafaro. Alternatively, the geodesicity property can be checked by verifying that the geodesic efficiency η_{GE} in Eq. (1) is equal to one. This is indeed the case since, essentially,

$$\cos^{-1} [|\langle m(t_A)|m(t_B)\rangle|] = \int_{t_A}^{t_B} \sqrt{\langle \dot{m}|\dot{m}\rangle} dt, \quad (36)$$

with $\cos^{-1} [|\langle m(t_A)|m(t_B)\rangle|] = |\theta(t_B) - \theta(t_A)|/2 = \int_{t_A}^{t_B} \sqrt{\langle \dot{m}|\dot{m}\rangle} dt$ given that $\langle \dot{m}|\dot{m}\rangle = \dot{\theta}^2/4$. Therefore, one can confirm that the evolution is a geodesic one. Finally, by construction (i.e., given the expression of the Hamiltonian $H(t) \stackrel{\text{def}}{=} i(|\dot{m}\rangle\langle m| - |m\rangle\langle \dot{m}|)$ as constructed in Ref. [21]), the evolution occurs with no waste of energy resources as well. In the nonstationary quantum evolution considered here, we obtained a geodesic path with a magnetic field $\mathbf{h}(t)$ in Eq. (34) that varies in magnitude and with a constant direction which is constantly perpendicular to the Bloch vector $\hat{a}(t)$ of the evolving quantum state $|m(t)\rangle$ in Eq. (32).

At this point, at the cost of wasting energy resources with $\eta_{\text{SE}} < 1$, we ask whether or not it is possible to have a vanishing curvature of the quantum evolution in an alternative magnetic field configuration where $\hat{a}(t) \cdot \mathbf{h}(t) \neq$

0, $\partial_t \hat{h}(t) \neq \mathbf{0}$, and $\partial_t \hat{a}(t) = 2\mathbf{h}(t) \times \hat{a}(t)$ continues to be satisfied. In other words, is it possible to generate a zero curvature and unit geodesic efficiency quantum evolution with an applied magnetic field that changes both in magnitude and direction which, in addition, is not constantly perpendicular to the Bloch vector of the evolving quantum state? We address this question in the next example.

B. Second example: $(\eta_{\text{GE}}, \eta_{\text{SE}}) = (1, < 1)$

In this second example, we assume to consider a quantum evolution governed by a nonzero trace nonstationary Hamiltonian given by $\mathbf{H}(t) \stackrel{\text{def}}{=} i(|\dot{m}\rangle \langle m| - |m\rangle \langle \dot{m}|) + \dot{\phi}|m\rangle \langle m|$ with a time-varying $\phi(t) \in \mathbb{R}$ and $|m(t)\rangle$ as in Eq. (32). From Ref. [21], we know that the Hamiltonians in the first and second example generate the same paths on the Bloch sphere. For this reason, the Bloch vector in this second example remains $\hat{a}(t) \stackrel{\text{def}}{=} (\sin(\theta) \cos(\varphi_0), \sin(\theta) \sin(\varphi_0), \cos(\theta))$. The Hamiltonian $\mathbf{H}(t)$ is such that $\mathbf{H}(t)(e^{-i\phi(t)}|m(t)\rangle) = i\partial_t(e^{-i\phi(t)}|m(t)\rangle)$. With respect to the computational basis $\{|0\rangle, |1\rangle\}$, the matrix representation of $\mathbf{H}(t)$ becomes

$$\mathbf{H}(t) = \begin{pmatrix} \dot{\phi} \cos^2(\frac{\theta}{2}) & \frac{e^{-i\varphi_0}}{2} [-i\dot{\theta} + \dot{\phi} \sin(\theta)] \\ \frac{e^{i\varphi_0}}{2} [i\dot{\theta} + \dot{\phi} \sin(\theta)] & \dot{\phi} \sin^2(\frac{\theta}{2}) \end{pmatrix}. \quad (37)$$

Then, setting $\mathbf{H}(t) = h_0(t)\mathbf{1} + \mathbf{h}(t) \cdot \boldsymbol{\sigma}$, we get that $h_0(t) \stackrel{\text{def}}{=} \dot{\phi}/2$ and

$$\mathbf{h}(t) \stackrel{\text{def}}{=} \begin{pmatrix} \frac{1}{2} \cos(\varphi_0) \sin(\theta) \dot{\phi} - \frac{1}{2} \sin(\varphi_0) \dot{\theta} \\ \frac{1}{2} \sin(\varphi_0) \sin(\theta) \dot{\phi} + \frac{1}{2} \cos(\varphi_0) \dot{\theta} \\ \frac{1}{2} \cos(\theta) \dot{\phi} \end{pmatrix}. \quad (38)$$

Note that when $\dot{\phi} = 0$, $\mathbf{h}(t)$ in Eq. (38) reduces to $\mathbf{h}(t)$ in Eq. (34). Furthermore, it can be explicitly checked that we correctly obtain that $\partial_t \hat{a}(t) = 2\mathbf{h}(t) \times \hat{a}(t)$ where $\hat{a}(t) \stackrel{\text{def}}{=} (\sin(\theta) \cos(\varphi_0), \sin(\theta) \sin(\varphi_0), \cos(\theta))$ and $\mathbf{h}(t)$ as in Eq. (38). Observe that in this second example, we have $\hat{a}(t) \cdot \mathbf{h}(t) = \dot{\phi}/2 \neq 0$, $\mathbf{h}^2(t) = (\dot{\phi}^2 + \dot{\theta}^2)/4$ is time-varying, and $\partial_t \hat{h}(t) \neq \mathbf{0}$. For simplicity of calculations, we assume in what follows that $\varphi_0 = 0$, $\phi(t) = \phi_0 + \Omega_0 t$, and $\theta(t) = \theta_0 + \omega_0 t$. This way, we have $\dot{\phi} = \Omega_0$ and $\dot{\theta} = \omega_0$. In these working assumptions, we have $\hat{a}(t) = \mathbf{a}(t) = (\sin(\theta), 0, \cos(\theta))$, $\mathbf{h}(t) = (\frac{\Omega_0}{2} \sin(\theta), \frac{\omega_0}{2}, \frac{\Omega_0}{2} \cos(\theta))$, and $\dot{\mathbf{h}}(t) = (\frac{\Omega_0 \omega_0}{2} \cos(\theta), 0, -\frac{\Omega_0 \omega_0}{2} \sin(\theta))$. Then, a straightforward but tedious calculation yields $\kappa_{\text{AC}}^2(\mathbf{a}, \mathbf{h}) = 0$, with the curvature coefficient defined in Eq. (35). This was expected since the evolution paths are the same as in the first example. Nevertheless, we checked the vanishing of the curvature coefficient to double-check the correctness of the expression in Eq. (35). For consistency check, one can also verify that $\eta_{\text{GE}} = 1$ in this second case as well. Interestingly, recalling that only $h_{\perp}(t)$ plays a key role in the calculation of the geodesic efficiency η_{GE} along with the fact that \mathbf{h} can be decomposed as $\mathbf{h} = \mathbf{h}_{\parallel} + \mathbf{h}_{\perp} = (\mathbf{h} \cdot \hat{a})\hat{a} + [\mathbf{h} - (\mathbf{h} \cdot \hat{a})\hat{a}]$, we observe that $(\mathbf{h}_{\perp})_{\text{case-2}} = (\mathbf{h}_{\perp})_{\text{case-1}} = (-(1/2)\sin(\varphi_0)\dot{\theta}, (1/2)\cos(\varphi_0)\dot{\theta}, 0)$. Finally, unlike the first example, we have $\eta_{\text{SE}}(t) = h_{\perp}(t) / \left[|h_0(t)| + \sqrt{h_{\parallel}^2(t) + h_{\perp}^2(t)} \right] < 1$. Specifically, it happens that $h_{\perp}^2(t) = \dot{\theta}^2/4$, $h_{\parallel}^2(t) = \dot{\phi}^2/4$, and $h_0(t) = \dot{\phi}/2$. Therefore, unlike the first example, this second example is specified by a nonzero trace Hamiltonian with $h_{\parallel}(t) \neq 0$. The departure from the traceless condition together with the emergence of a component of the magnetic field along the Bloch vector $\hat{a}(t)$ lead to a quantum evolution in which energy resources are wasted, despite being a geodesic evolution.

In summary, in these first two examples, we have used Uzdin's formalism to show two main points. First, unlike in a stationary setting, in a nonstationary setting it is not necessary to have $\hat{a}(t) \cdot \mathbf{h}(t) = 0$ for having a geodesic evolution. Second, a geodesic path can be energetically wasteful. In this next pair of examples, we show that it is not sufficient to have $\hat{a}(t) \cdot \mathbf{h}(t) = 0$ in a nonstationary setting in order to produce a geodesic quantum evolution. Moreover, we shall see that given a wasteful Hamiltonian specified by a magnetic field with a high intensity, it is possible to create a new Hamiltonian that generates the same paths on the Bloch sphere as the original Hamiltonian, while mitigating the energy waste by removing unuseful parts of the original magnetic field and lowering its intensity (in an effort to drive $h_{\parallel} \rightarrow 0$). We are now ready to discuss the next two examples.

C. Third example: $(\eta_{\text{GE}}, \eta_{\text{SE}}) = (< 1, < 1)$

To begin, we observe that the constant Hamiltonians $\mathbf{H}_{\text{sub-opt}}(\alpha)$ with $\alpha \neq \pi/2$ in Eq. (17) lead to quantum evolutions with $(\eta_{\text{GE}}, \eta_{\text{SE}}) = (< 1, < 1)$. In particular, given $\Delta E(\alpha)$ calculated in Appendix A, the speed efficiency

Example	$\bar{\eta}_{\text{GE}}$	$\bar{\eta}_{\text{SE}}$	η_{HE}	Type of quantum evolution
First	1	1	1	Geodesic un wasteful
Second	1	~ 0.87	~ 0.87	Geodesic wasteful
Third	~ 0.98	$\sqrt{3}/2$	~ 0.85	Nongeodesic wasteful
Fourth	~ 0.98	1	~ 0.98	Nongeodesic un wasteful

TABLE II: Numerical estimates of the average geodesic efficiency, average speed efficiency, and hybrid efficiency. Time-averages are estimated over the unit time interval. In the second example, we assume $\theta(t) \stackrel{\text{def}}{=} \omega_0 t$ and $\phi(t) \stackrel{\text{def}}{=} \nu_0 t$. For simplicity, we set $\omega_0 = 1$ and $\nu_0 = 10^{-1}$ in the numerical calculations. Moreover, in the third and fourth examples, we put $\gamma = 1$. Finally, physical units are determined so that the reduced Planck constant can be set equal to one.

in Eq. (6) reduces to $\eta_{\text{SE}}(\alpha) = \Delta E(\alpha)/E = \sqrt{1 - \cos^2(\alpha) \cos^2(\theta_{AB}/2)}$. For this reason, we consider in this third example a quantum evolution specified by a time-independent Hamiltonian given by $H \stackrel{\text{def}}{=} \mathbf{h} \cdot \boldsymbol{\sigma} = \gamma \sigma_z$, with $\mathbf{h} = \gamma \hat{z}$ and $\gamma > 0$. Furthermore, we assume that the initial state is given by $|A\rangle \stackrel{\text{def}}{=} (\sqrt{3}/2)|0\rangle + (1/2)|1\rangle$ with $\rho_A \stackrel{\text{def}}{=} |A\rangle\langle A| = (\mathbf{1} + \hat{a} \cdot \boldsymbol{\sigma})/2$. The unit Bloch vector equals $\hat{a} \stackrel{\text{def}}{=} (\sqrt{3}/2)\hat{x} + (1/2)\hat{z}$ and is such that $\hat{a} \cdot \mathbf{h} \neq 0$. The action of the unitary time propagator $U(t) = e^{-iHt}$ on $|A\rangle$ yields

$$|\psi(t)\rangle = e^{-i\gamma t} \left[\frac{\sqrt{3}}{2}|0\rangle + \frac{1}{2}e^{i2\gamma t}|1\rangle \right]. \quad (39)$$

We can notice from Eq. (39) that, apart for a global phase factor that is not relevant when considering the evolution on the Bloch sphere, the only parameter that changes is the azimuthal angle φ according to $\varphi = \varphi(t) \stackrel{\text{def}}{=} 2\gamma t$. This is in agreement with the fact that the operator $e^{-i\gamma\sigma_z t}$ corresponds to a rotation of angle $2\gamma t$ around the axis \hat{z} in the Bloch sphere. A straightforward calculation yields $\kappa_{\text{AC}}^2(\mathbf{a}, \mathbf{h}) \stackrel{\text{def}}{=} 4(\mathbf{a} \cdot \mathbf{h})^2 / [\mathbf{h}^2 - (\mathbf{a} \cdot \mathbf{h})^2] = 4/3 \neq 0$ and $\eta_{\text{GE}} \stackrel{\text{def}}{=} s_0/s \leq 1$ evaluated between $|A\rangle$ and $|\psi(t)\rangle$ given by,

$$\eta_{\text{GE}} = \frac{2}{\sqrt{3}} \frac{\arccos\left(\frac{\sqrt{[3+\cos(2\gamma t)]^2 + \sin^2(2\gamma t)}}{4}\right)}{\gamma t}. \quad (40)$$

Therefore, this quantum evolution is nongeodesic. Furthermore, we can explicitly verify that the speed efficiency $\eta_{\text{SE}} \stackrel{\text{def}}{=} \Delta H_\rho / \|\mathbf{H}\|_{\text{SP}}$ of this evolution is smaller than 1. Indeed, since $\Delta H_\rho^2 = (3/4)\gamma^2$ and $\|\mathbf{H}\|_{\text{SP}}^2 = \gamma^2$, we find $\eta_{\text{SE}} = \sqrt{3}/2 < 1$. In conclusion, the quantum evolution considered is neither geodesic nor energy-resourceful.

In our final example, starting from the time-independent Hamiltonian of this third example, we construct a new time-dependent Hamiltonian that generates the same evolution paths on the Bloch sphere (i.e., same nonvanishing curvature coefficient κ_{AC}^2 and same non-unit geodesic efficiency η_{GE}), but with no waste of energy resources (i.e., $\eta_{\text{SE}} = 1$).

D. Fourth example: $(\eta_{\text{GE}}, \eta_{\text{SE}}) = (< 1, 1)$

We construct here a traceless time-dependent Hamiltonian with 100% speed efficiency following Uzdin's prescription. The Hamiltonian is given by $H(t) = i(|\partial_t m\rangle\langle m| - |m\rangle\langle \partial_t m|)$, where $|m\rangle$ is the parallel transported vector defined in terms of $|\psi(t)\rangle$ in Eq. (39) as

$$|m(t)\rangle \stackrel{\text{def}}{=} e^{-\int_0^t \langle \psi(t') | \partial_{t'} \psi(t') \rangle dt'} |\psi(t)\rangle, \quad (41)$$

with $\partial_{t'} \stackrel{\text{def}}{=} \partial/\partial t'$. Exploiting the time-dependent Schrödinger evolution equation $i\partial_t |\psi(t)\rangle = H(t) |\psi(t)\rangle$ to evaluate the integral in Eq. (41), $|m(t)\rangle$ becomes

$$|m(t)\rangle = \frac{\sqrt{3}}{2} e^{-i\frac{\gamma}{2}t} |0\rangle + \frac{1}{2} e^{i\frac{3\gamma}{2}t} |1\rangle. \quad (42)$$

Note that from Eq. (42) we could write $|m(t)\rangle_{\text{case-4}} = e^{i\frac{\gamma}{2}t} |m(t)\rangle_{\text{case-3}}$, using Eq. (39) on the right-hand side. From Eq. (42), we can easily check that $\langle m(t) | m(t) \rangle = 1$ and $\langle m(t) | \partial_t m(t) \rangle = 0$. Using Eq. (42), $H(t)$ can be recast as

$$H(t) = \frac{3}{4}\gamma |0\rangle\langle 0| - \frac{\sqrt{3}}{4}\gamma e^{i2\gamma t} |1\rangle\langle 0| - \frac{\sqrt{3}}{4}\gamma e^{-i2\gamma t} |0\rangle\langle 1| - \frac{3}{4}\gamma |1\rangle\langle 1|. \quad (43)$$

In terms of the expression $H(t) = \mathbf{h}(t) \cdot \boldsymbol{\sigma}$, $H(t)$ in Eq. (43) is specified by $\mathbf{h}(t) \stackrel{\text{def}}{=} \frac{\sqrt{3}}{2} \gamma \hat{h}(t)$, with $\hat{h}(t)$ given by

$$\hat{h}(t) \stackrel{\text{def}}{=} \left(-\frac{1}{2} \cos(2\gamma t), -\frac{1}{2} \sin(2\gamma t), \frac{\sqrt{3}}{2} \right). \quad (44)$$

Comparing $(\mathbf{h})_{\text{case-3}} \stackrel{\text{def}}{=} \gamma \hat{z}$ with $(\mathbf{h})_{\text{case-4}} \stackrel{\text{def}}{=} (\sqrt{3}/2) \gamma \hat{h}(t)$, we note that the magnitude of the magnetic field in case-4 is smaller than the magnitude of the magnetic field in case-3. Interestingly, we note that the time-dependent unit Bloch vector $\hat{a}(t)$ that corresponds to the states $|\psi(t)\rangle$ and $|m(t)\rangle$ in Eqs. (39) and (42), respectively, is given by

$$\hat{a}(t) \stackrel{\text{def}}{=} \left(\frac{\sqrt{3}}{2} \cos(2\gamma t), \frac{\sqrt{3}}{2} \sin(2\gamma t), \frac{1}{2} \right). \quad (45)$$

From Eqs. (44) and (45), it is straightforward to verify that $\hat{a}(t) \perp \hat{h}(t)$. Therefore, since \mathbf{h} can be decomposed as $\mathbf{h} = \mathbf{h}_{\parallel} + \mathbf{h}_{\perp} = (\mathbf{h} \cdot \hat{a}) \hat{a} + [\mathbf{h} - (\mathbf{h} \cdot \hat{a}) \hat{a}]$ and given that $\eta_{\text{SE}}(t) = h_{\perp}(t) / \sqrt{h_{\parallel}^2(t) + h_{\perp}^2(t)}$, we have in our case here that $h_{\parallel}(t) = 0$ and $\eta_{\text{SE}}(t)$ is identically equal to one. In conclusion, we can interpret the waste in energy resources in terms of the presence of useless parallel magnetic field when comparing case-3 with case-4. Finally, given $\mathbf{h}(t) \stackrel{\text{def}}{=} \frac{\sqrt{3}}{2} \gamma \hat{h}(t)$ and $\hat{a}(t)$ in Eq. (45), we note that $\hat{a}(t) \cdot \mathbf{h}(t) = 0$, $\hat{a}(t) \cdot \dot{\mathbf{h}}(t) = 0$, and $\mathbf{h}(t) \cdot \dot{\mathbf{h}}(t) = 0$. Therefore, the cumbersome expression of the curvature coefficient in Eq. (35) reduces to $\kappa_{\text{AC}}^2(\mathbf{a}, \mathbf{h}) = \dot{\mathbf{h}}^2(t) / \mathbf{h}^4(t) = 4/3$. This result coincides, as expected, with the result obtained in the third example presented earlier. As a final remark, based on what we have shown in this example, we stress that in a nonstationary setting (unlike the stationary setting), the condition $\hat{a}(t) \cdot \mathbf{h}(t) = 0$ is not generally sufficient to yield a geodesic quantum evolution. It becomes sufficient only when \mathbf{h} and $\dot{\mathbf{h}}$ are collinear (i.e., when \mathbf{h} does not change in direction). This can also be seen in a very neat manner as follows. When $\mathbf{a} \cdot \mathbf{h} = 0$ (with $\mathbf{a} = \hat{a}$), $\dot{\mathbf{a}} \cdot \mathbf{h} + \mathbf{a} \cdot \dot{\mathbf{h}} = 0$. Then, since $\dot{\mathbf{a}} = 2\mathbf{h} \times \mathbf{a}$ implies $\dot{\mathbf{a}} \cdot \mathbf{h} = 0$, we have $\mathbf{a} \cdot \dot{\mathbf{h}} = 0$. Then, $\kappa_{\text{AC}}^2(\mathbf{a}, \mathbf{h})$ in Eq. (35) reduces to

$$\kappa_{\text{AC}}^2(\mathbf{a}, \mathbf{h}) = \frac{\mathbf{h}^2 \dot{\mathbf{h}}^2 - (\mathbf{h} \cdot \dot{\mathbf{h}})^2}{[\mathbf{h}^2 - (\mathbf{a} \cdot \mathbf{h})^2]^3}. \quad (46)$$

Setting $\mathbf{h} = \mathbf{h}_{\perp} = h_{\perp}(t) \hat{h}_{\perp}(t)$ (since $\mathbf{h}_{\parallel} = \mathbf{0}$, given that $\mathbf{a} \cdot \mathbf{h} = 0$), after some algebra, Eq. (46) can be recast as

$$\kappa_{\text{AC}}^2(t) = \frac{\frac{d\hat{h}_{\perp}}{dt} \cdot \frac{d\hat{h}_{\perp}}{dt}}{\mathbf{h}_{\perp}^2}. \quad (47)$$

From Eq. (47), it is evident that $\kappa_{\text{AC}}^2(t)$ vanishes in a time-dependent setting with $\mathbf{a} \cdot \mathbf{h} = 0$ if and only if the magnetic field does not change in direction. With this remark, we end our presentation of these four illustrative examples. A summary of the numerical estimates of the average geodesic efficiency, average speed efficiency, and hybrid efficiency for each one of the four examples considered here are presented in Table II.

We are now ready for our summary of results and final considerations.

V. CONCLUDING REMARKS

In this paper, we investigated different families of sub-optimal qubit Hamiltonians, both stationary (Eq.(17)) and time-varying (Eqs. (27) and (29)), for which the so-called geodesic efficiency (Eq. (1)) and the speed efficiency (Eq. (6)) of the corresponding quantum evolutions are less than one. The detrimental effects caused by the stationary and nonstationary Hamiltonians and quantified by means of the geodesic and speed efficiency, respectively, are illustrated in Figs. 3 and 4 (stationary case) and Figs. 5 and 6 (nonstationary case). In addition, we proposed a different hybrid efficiency measure (Eq. (13)) that combines the two efficiency measures mentioned earlier. As reported in Table I, this hybrid efficiency quantifier allows us to categorize quantum evolutions into four groups: Geodesic unwasteful, nongeodesic unwasteful, geodesic wasteful, and nongeodesic wasteful. Then, for each and everyone of these groups, we exhibited practical illustrative examples that demonstrate how this hybrid measure captures the overall deviations from optimal timing and perfect speed efficiency within a specific time-frame. As summary of results appears in Table II. Ultimately, after considering the notion of curvature in quantum evolution (Eq. (35)), we explored Hamiltonians that

are determined by magnetic field arrangements, whether they are stationary or nonstationary. These Hamiltonians result in an optimal hybrid efficiency, incorporating both time-optimality and 100% speed efficiency, within a finite time period.

The main conclusions that can be derived are as follows. First, the geodesic efficiency η_{GE} is a global efficiency indicator that quantifies quantum Hamiltonian evolutions in terms of departures from paths of shortest length [9]. Furthermore, as we have explicitly shown, it depends in an essential manner only on the transverse magnetic field vector $\mathbf{h}_\perp(t)$ that specifies the magnetic field vector $\mathbf{h}(t) \stackrel{\text{def}}{=} \mathbf{h}_\parallel(t) + \mathbf{h}_\perp(t)$ in the Hamiltonian $H(t) \stackrel{\text{def}}{=} \mathbf{h}(t) \cdot \boldsymbol{\sigma}$. Second, the speed efficiency η_{SE} is a local efficiency quantifier that characterizes quantum evolutions in terms of deviations from paths of minimal waste of energy [21]. Furthermore, unlike η_{GE} , we have demonstrated that it depends on both the parallel and the transverse magnetic field vectors $\mathbf{h}_\parallel(t)$ and $\mathbf{h}_\perp(t)$, respectively, that define the magnetic field vector $\mathbf{h}(t) \stackrel{\text{def}}{=} \mathbf{h}_\parallel(t) + \mathbf{h}_\perp(t)$ in the Hamiltonian $H(t) \stackrel{\text{def}}{=} \mathbf{h}(t) \cdot \boldsymbol{\sigma}$. Third, for stationary evolutions, unit geodesic efficiency Hamiltonian evolutions are characterized by magnetic field vectors $\mathbf{h}(t)$ that are constantly orthogonal to the Bloch vector $\mathbf{a}(t)$ of the evolving state vector $|\psi(t)\rangle$. In the time-varying case, instead, the condition $\mathbf{a}(t) \cdot \mathbf{h}(t) = \mathbf{0}$ is neither necessary (see the Fourth Example), nor sufficient (see the Second Example) to achieve geodesicity. Fourth, in both stationary and nonstationary Hamiltonian evolutions, nonzero trace Hamiltonians $H(t) \stackrel{\text{def}}{=} h_0(t)\mathbf{1} + \mathbf{h}(t) \cdot \boldsymbol{\sigma}$ are necessarily energy wasteful. Instead, traceless Hamiltonians $H(t) \stackrel{\text{def}}{=} \mathbf{h}(t) \cdot \boldsymbol{\sigma}$ for which the parallel magnetic field vector $\mathbf{h}_\parallel(t)$ of the magnetic field $\mathbf{h}(t)$ vanishes are not energy wasteful. Fifth, the notion of hybrid efficiency η_{HE} offers a new perspective on quantum evolutions, encompassing both time-optimality and energy-optimality. In particular, it suggests clever ways to calculate the curvature coefficient κ_{AC}^2 of quantum evolutions [32, 33] by exploiting ideas from Uzdin’s speed efficiency theoretical setting. Based on these findings, we have determined that a practical approach to achieving quantum evolutions with unit hybrid efficiency using time-dependent Hamiltonians involves a transverse magnetic field that varies only in intensity, not direction. Furthermore, thinking in terms of hybrid efficiency η_{HE} offers efficient ways to construct speed efficient quantum evolutions starting from more speed inefficient quantum evolutions, while preserving the same level of geodesic efficiency η_{GE} . Again, this is achieved by mixing together ideas from Uzdin’s speed efficiency theoretical setting with concepts from the Anandan-Aharonov geometric approach to quantum evolutions as illustrated in our work.

We see three clear research lines that can originate from the limitations of our investigation. A first one would be the nontrivial extension of our ideas to multi-level quantum systems in pure states [34–39]. A second one would be shifting the focus on quantum evolutions inside the Bloch sphere, where quantum systems are in mixed quantum states. In this context, one of the issues could be the choice of the “proper” metric [40–47]. A third one, the most intriguing in our view, would be studying the behavior of the complexity of quantum evolutions [48–55] (even for two-level systems) in terms of deviations from ideality specified by curvature and efficiency concepts like the ones used in this paper. In this context, the pertinent findings derived from some of the concepts presented in our current work are already being successfully implemented in Refs. [29] and [30].

In conclusion, despite the current limitations, we are firmly convinced that our study will motivate other scholars and pave the way for further comprehensive investigations into the relationship between geometry and quantum mechanics where the concept of efficiency plays a significant role.

Acknowledgments

The authors express their gratitude to the anonymous Referees for their constructive feedback, which has contributed to the enhancement of the paper. Any opinions, findings and conclusions or recommendations expressed in this material are those of the author(s) and do not necessarily reflect the views of their home Institutions.

-
- [1] R. P. Feynman, F. Vernon, and R. W. Hellwarth, *Geometrical representation of the Schrödinger equation for solving maser problems*, J. Appl. Phys. **28**, 49 (1957).
 - [2] J. P. Provost and G. Vallee, *Riemannian structure on manifolds of quantum states*, Commun. Math. Phys. **76**, 289 (1980).
 - [3] W. K. Wootters, *Statistical distance and Hilbert space*, Phys. Rev. **D23**, 357 (1981).
 - [4] N. Mukunda and R. Simon, *Quantum kinematic approach to the geometric phase I. General Formalism*, Annals of Physics **228**, 205 (1993).

- [5] S. L. Braunstein and C. M. Caves, *Statistical distance and the geometry of quantum states*, Phys. Rev. Lett. **72**, 3439 (1994).
- [6] S. L. Braunstein and C. M. Caves, *Geometry of quantum states*. In: B. V. Belavkin, O. Hirota, and R. L. Hudson (eds.), Quantum Communications and Measurement, pp. 21-30. Springer, Boston, MA (1995).
- [7] I. Bengtsson and K. Życzkowski, *Geometry of Quantum States*, Cambridge University Press (2006).
- [8] A. Uhlmann and B. Crell, *Geometry of state spaces*, Lecture Notes in Physics **768**, 1 (2009).
- [9] J. Anandan and Y. Aharonov, *Geometry of quantum evolution*, Phys. Rev. Lett. **65**, 1697 (1990).
- [10] D. C. Brody, *Elementary derivation for passage times*, J. Phys. A: Math. Gen. **36**, 5587 (2003).
- [11] A. Carlini, A. Hosoya, T. Koike, and Y. Okudaira, *Time-optimal quantum evolution*, Phys. Rev. Lett. **96**, 060503 (2006).
- [12] D. C. Brody and D. W. Hook, *On optimum Hamiltonians for state transformations*, J. Phys. A: Math. Gen. **39**, L167 (2006).
- [13] D. C. Brody and D. W. Hook, *On optimum Hamiltonians for state transformation*, J. Phys. A: Math. Theor. **40**, 10949 (2007).
- [14] C. M. Bender, D. C. Brody, H. F. Jones, and B. K. Meister, *Faster than Hermitian quantum mechanics*, Phys. Rev. Lett. **98**, 040403 (2007).
- [15] C. M. Bender and D. C. Brody, *Optimal time evolution for Hermitian and non-Hermitian Hamiltonians*, Lecture Notes in Physics **789**, 341 (2009).
- [16] A. Mostafazadeh, *Hamiltonians generating optimal-speed evolutions*, Phys. Rev. **A79**, 014101 (2009).
- [17] C. Cafaro and P. M. Alsing, *Qubit geodesics on the Bloch sphere from optimal-speed Hamiltonian evolutions*, Class. Quantum Grav. **40**, 115005 (2023).
- [18] E. Barnes, X. Wang, and S. D. Sarma, *Robust quantum control using smooth pulses and topological winding*, Scientific Reports **5**, 12685 (2015).
- [19] A. Vezvaei, G. Sharma, S. E. Economou, and E. Barnes, *Driven dynamics of a quantum dot electron spin coupled to bath of higher-spin nuclei*, Phys. Rev. **B103**, 235301 (2021).
- [20] J. S. Van Dyke et al., *Protecting quantum information in quantum dot spin chains by driving exchange interactions periodically*, Phys. Rev. **B103**, 245303 (2021).
- [21] R. Uzdin, U. Günther, S. Rahav, and N. Moiseyev, *Time-dependent Hamiltonians with 100% evolution speed efficiency*, J. Phys. A: Math. Theor. **45**, 415304 (2012).
- [22] R. Uzdin, A. Levy, and R. Kosloff, *Equivalence of quantum heat machines, and quantum-thermodynamic signatures*, Phys. Rev. **X5**, 031044 (2015).
- [23] F. Campaioli, W. Sloan, K. Modi, and F. A. Pollok, *Algorithm for solving unconstrained unitary quantum brachistochrone problems*, Phys. Rev. **A100**, 062328 (2019).
- [24] J. Xu et al., *Balancing the quantum speed limit and instantaneous energy cost in adiabatic quantum evolution*, Chinese Phys. Lett. **41**, 040202 (2024).
- [25] M. H. Tahar and F. Meot, *Tune compensation in nearly scaling fixed field alternating gradient accelerators*, Phys. Rev. Accel. and Beams **23**, 054003 (2020).
- [26] J. Debnath et al., *Optimization of compensation of magnetic field imperfection in K500 superconducting cyclotron*, Journal of Instrumentation **15**, T09004 (2020).
- [27] S. Xu, J. Li, Z. Zhou, K. Ding, and Y. Chen, *Effects of the spatial offsets of superconducting coils on the magnetic field in SC200 cyclotron*, IEEE Transaction on Applied Superconductivity **32**, 4901908 (2022).
- [28] R. G. Sharma, *Superconductivity: Basics and Applications to Magnets*, Springer Nature Switzerland AG (2021).
- [29] C. Cafaro, L. Rossetti, and P. M. Alsing, *Curvature of quantum evolutions for qubits in time-dependent magnetic fields*, Phys. Rev. **A111**, 012408 (2025).
- [30] C. Cafaro, L. Rossetti, and P. M. Alsing, *Complexity of quantum-mechanical evolutions from probability amplitudes*, Nuclear Physics **B1010**, 116755 (2025).
- [31] C. Cafaro, S. Ray, and P. M. Alsing, *Geometric aspects of analog quantum search evolutions*, Phys. Rev. **A102**, 052607 (2020).
- [32] P. M. Alsing and C. Cafaro, *From the classical Frenet–Serret apparatus to the curvature and torsion of quantum-mechanical evolutions. Part I. Stationary Hamiltonians*, Int. J. Geom. Methods Mod. Phys. **21**, 2450152 (2024).
- [33] P. M. Alsing and C. Cafaro, *From the classical Frenet–Serret apparatus to the curvature and torsion of quantum-mechanical evolutions. Part II. Nonstationary Hamiltonians*, Int. J. Geom. Methods Mod. Phys. **21**, 2450151 (2024).
- [34] L. Jakobczyk and M. Siennicki, *Geometry of Bloch vectors in two-qubit system*, Phys. Lett. **A286**, 383 (2001).
- [35] G. Kimura, *The Bloch vector for N-level systems*, Phys. Lett. **A314**, 339 (2003).
- [36] R. A. Bertlmann and P. Krammer, *Bloch vectors for qudits*, J. Phys. A: Math. Theor. **41**, 235303 (2008).
- [37] P. Kurzynski, *Multi-Bloch vector representation of the qutrit*, Quantum Inf. Comp. **11**, 361 (2011).
- [38] J. Xie et al., *Observing geometry of quantum states in a three-level system*, Phys. Rev. Lett. **125**, 150401 (2020).
- [39] C. Eltschka, M. Huber, S. Morelli, and J. Siewert, *The shape of higher-dimensional state space: Bloch-ball analog for a qutrit*, Quantum **5**, 485 (2021).
- [40] D. Bures, *An extension of Kakutani’s theorem on infinite product measures to the tensor product of semifinite ω^* -algebras*, Trans. Amer. Math. Soc. **135**, 199 (1969).
- [41] A. Uhlmann, *The “transition probability” in the state space of a $*$ -algebra*, Rep. Math. Phys. **9**, 273 (1976).
- [42] M. Hübner, *Explicit computation of the Bures distance for density matrices*, Phys. Lett. **A163**, 239 (1992).
- [43] E. Sjöqvist, *Geometry along evolution of mixed quantum states*, Phys. Rev. Research **2**, 013344 (2020).
- [44] N. Hornedal, D. Allan, and O. Sonnerborn, *Extensions of the Mandelstam–Tamm quantum speed limit to systems in mixed*

- states, *New J. Phys.* **24**, 055004 (2022).
- [45] C. Cafaro and P. M. Alsing, *Bures and Sjöqvist metrics over thermal state manifolds for spin qubits and superconducting flux qubits*, *Eur. Phys. J. Plus* **138**, 655 (2023).
- [46] P. M. Alsing, C. Cafaro, D. Felice, and O. Luongo, *Geometric aspects of mixed quantum states inside the Bloch sphere*, *Quantum Reports* **6**, 90 (2024).
- [47] A. Naderzadeh-ostad and S. J. Akhtarshenas, *Optimal quantum speed for mixed states*, *J. Phys. A: Math. Theor.* **57**, 075301 (2024).
- [48] A. R. Brown, L. Susskind, and Y. Zhao, *Quantum complexity and negative curvature*, *Phys. Rev.* **D95**, 045010 (2017).
- [49] S. Chapman, M. P. Heller, H. Marrachio, and F. Pastawski, *Toward a definition of complexity for quantum field theory states*, *Phys. Rev. Lett.* **120**, 121602 (2018).
- [50] A. R. Brown and L. Susskind, *Complexity geometry of a single qubit*, *Phys. Rev.* **D100**, 046020 (2019).
- [51] R. Auzzi, S. Baiguera, G. B. De Luca, A. Legramandi, G. Nardelli, and N. Zenoni, *Geometry of quantum complexity*, *Phys. Rev.* **D103**, 106021 (2021).
- [52] C. Cafaro, S. Ray, and P. M. Alsing, *Complexity and efficiency of minimum entropy production probability paths from quantum dynamical evolutions*, *Phys. Rev.* **E105**, 034143 (2022).
- [53] V. Balasubramanian, P. Caputa, J. M. Magan, and Q. Wu, *Quantum chaos and the complexity of spread of states*, *Phys. Rev.* **D106**, 046007 (2022).
- [54] C. Cafaro and P. M. Alsing, *Complexity of pure and mixed qubit geodesic paths on curved manifolds*, *Phys. Rev.* **D106**, 096004 (2022).
- [55] A. A. Nizami and A. W. Shrestha, *Krylov construction and complexity for driven quantum systems*, *Phys. Rev.* **E108**, 054222 (2023).
- [56] J. Samuel and R. Bhandari, *General setting for Berry's phase*, *Phys. Rev. Lett.* **60**, 2339 (1988).
- [57] P. M. Alsing, C. Cafaro, O. Luongo, C. Lupo, S. Mancini, and H. Quevedo, *Comparing metrics for mixed quantum states: Sjöqvist and Bures*, *Phys. Rev.* **A107**, 052411 (2023).
- [58] J. Alvarez-Vizoso, R. Arn, M. Kirby, C. Peterson, and B. Draper, *Geometry of curves in \mathbb{R}^n from the local singular value decomposition*, *Lin. Algebra Appl.* **571**, 180 (2019).
- [59] R. Millman and G. Parker, *Elements of Differential Geometry*, Prentice Hall, NY (1977).

Appendix A: Calculation of ΔE

In this Appendix, we present a non-geometric calculation of the energy uncertainty $\Delta E(\alpha)$ introduced in the first subsection of Section III by means of ordinary quantum-mechanical rules.

Remember that the energy uncertainty ΔE is defined as

$$\Delta E \stackrel{\text{def}}{=} \sqrt{\langle H_{\text{sub-opt}}^2 \rangle - \langle H_{\text{sub-opt}} \rangle^2} = \sqrt{\text{tr}(\rho H_{\text{sub-opt}}^2) - [\text{tr}(\rho H_{\text{sub-opt}})]^2}. \quad (\text{A1})$$

Furthermore, recall that the sub-optimal Hamiltonian $H_{\text{sub-opt}}$ in Eq. (A1) is given by,

$$H_{\text{sub-opt}} \stackrel{\text{def}}{=} E \left[\cos(\alpha) \frac{\hat{a} + \hat{b}}{2 \cos(\frac{\theta_{AB}}{2})} + \sin(\alpha) \frac{\hat{a} \times \hat{b}}{\sin(\theta_{AB})} \right] \cdot \boldsymbol{\sigma}, \quad (\text{A2})$$

with $\cos(\theta_{AB}) = \hat{a} \cdot \hat{b}$. Using standard properties of the Pauli matrices together with the identity $(\vec{a} \cdot \boldsymbol{\sigma})(\vec{b} \cdot \boldsymbol{\sigma}) = (\vec{a} \cdot \vec{b}) \mathbf{1} + i(\vec{a} \times \vec{b}) \cdot \boldsymbol{\sigma}$ for any pair of vectors \vec{a} and \vec{b} in \mathbb{R}^3 , we proceed with the calculation of expectation values with respect to the initial state $|A\rangle$ with $\rho \stackrel{\text{def}}{=} |A\rangle\langle A| = (\mathbf{1} + \hat{a} \cdot \boldsymbol{\sigma})/2$. We note that,

$$\begin{aligned} \langle H_{\text{sub-opt}} \rangle &= \text{tr}(\rho H_{\text{sub-opt}}) \\ &= \text{tr} \left\{ \left(\frac{\mathbf{1} + \hat{a} \cdot \boldsymbol{\sigma}}{2} \right) E \left[\cos(\alpha) \frac{\hat{a} + \hat{b}}{2 \cos(\frac{\theta_{AB}}{2})} + \sin(\alpha) \frac{\hat{a} \times \hat{b}}{\sin(\theta_{AB})} \right] \cdot \boldsymbol{\sigma} \right\} \\ &= \text{tr} \left[\left(\frac{\mathbf{1} + \hat{a} \cdot \boldsymbol{\sigma}}{2} \right) \frac{E \cos(\alpha)}{2 \cos(\frac{\theta_{AB}}{2})} (\hat{a} + \hat{b}) \cdot \boldsymbol{\sigma} \right] + \text{tr} \left[\left(\frac{\mathbf{1} + \hat{a} \cdot \boldsymbol{\sigma}}{2} \right) \frac{E \sin(\alpha)}{\sin(\theta_{AB})} (\hat{a} \times \hat{b}) \cdot \boldsymbol{\sigma} \right] \\ &= \text{tr} \left\{ \frac{E \cos(\alpha)}{4 \cos(\frac{\theta_{AB}}{2})} [(\hat{a} \cdot \boldsymbol{\sigma}) ((\hat{a} + \hat{b}) \cdot \boldsymbol{\sigma})] \right\} \\ &= \frac{E \cos(\alpha)}{4 \cos(\frac{\theta_{AB}}{2})} \text{tr} \left\{ \hat{a} \cdot (\hat{a} + \hat{b}) \mathbf{1} + \hat{a} \times (\hat{a} + \hat{b}) \cdot \boldsymbol{\sigma} \right\} \\ &= \frac{E \cos(\alpha)}{2 \cos(\frac{\theta_{AB}}{2})} [\hat{a} \cdot (\hat{a} + \hat{b})]. \end{aligned} \quad (\text{A3})$$

Therefore, from Eq. (A3), $\langle H_{\text{sub-opt}} \rangle^2$ reduces to

$$\begin{aligned} \langle H_{\text{sub-opt}} \rangle^2 &= \left[\frac{E \cos(\alpha)}{2 \cos(\frac{\theta_{AB}}{2})} \right]^2 [\hat{a} \cdot (\hat{a} + \hat{b})]^2 \\ &= \frac{E^2 \cos^2(\alpha)}{4 \cos^2(\frac{\theta_{AB}}{2})} (\hat{a} \cdot \hat{a} + \hat{a} \cdot \hat{b})^2 \\ &= \frac{E^2 \cos^2(\alpha)}{4 \cos^2(\frac{\theta_{AB}}{2})} [1 + \cos(\theta_{AB})]^2 \\ &= \frac{E^2 \cos^2(\alpha)}{4 \cos^2(\frac{\theta_{AB}}{2})} \left[2 \cos^2\left(\frac{\theta_{AB}}{2}\right) \right]^2 \\ &= E^2 \cos^2(\alpha) \cos^2\left(\frac{\theta_{AB}}{2}\right), \end{aligned} \quad (\text{A4})$$

that is,

$$\langle H_{\text{sub-opt}} \rangle^2 = E^2 \cos^2(\alpha) \cos^2\left(\frac{\theta_{AB}}{2}\right). \quad (\text{A5})$$

Furthermore, following a similar line of reasoning, we have

$$\begin{aligned}
H_{\text{sub-opt}}^2 &= \frac{E^2 \cos^2(\alpha)}{4 \cos\left(\frac{\theta_{AB}}{2}\right)} \left[(\hat{a} + \hat{b}) \cdot \boldsymbol{\sigma} \right] \left[(\hat{a} + \hat{b}) \cdot \boldsymbol{\sigma} \right] + \\
&+ \frac{E^2 \sin^2(\alpha)}{\sin^2(\theta_{AB})} \left[(\hat{a} \times \hat{b}) \cdot \boldsymbol{\sigma} \right] \left[(\hat{a} \times \hat{b}) \cdot \boldsymbol{\sigma} \right] + \\
&+ \frac{E^2 \sin(\alpha) \cos(\alpha)}{2 \sin(\theta_{AB}) \cos\left(\frac{\theta_{AB}}{2}\right)} \left\{ \left[(\hat{a} + \hat{b}) \cdot \boldsymbol{\sigma} \right] \left[(\hat{a} \times \hat{b}) \cdot \boldsymbol{\sigma} \right] + \left[(\hat{a} \times \hat{b}) \cdot \boldsymbol{\sigma} \right] \left[(\hat{a} + \hat{b}) \cdot \boldsymbol{\sigma} \right] \right\} \\
&= \frac{E^2 \cos^2(\alpha)}{4 \cos\left(\frac{\theta_{AB}}{2}\right)} (\hat{a} + \hat{b})^2 \mathbf{1} + \frac{E^2 \sin^2(\alpha)}{\sin^2(\theta_{AB})} (\hat{a} \times \hat{b})^2 \mathbf{1} + \frac{E^2 \sin(\alpha) \cos(\alpha)}{2 \sin(\theta_{AB}) \cos\left(\frac{\theta_{AB}}{2}\right)} \\
&\cdot \left[(\hat{a} + \hat{b}) \cdot (\hat{a} \times \hat{b}) \mathbf{1} + i \left((\hat{a} + \hat{b}) \times (\hat{a} \times \hat{b}) \right) \cdot \boldsymbol{\sigma} + \right. \\
&\quad \left. + (\hat{a} \times \hat{b}) \cdot (\hat{a} + \hat{b}) \mathbf{1} + i \left((\hat{a} \times \hat{b}) \times (\hat{a} + \hat{b}) \right) \cdot \boldsymbol{\sigma} \right] \\
&= \frac{E^2 \cos^2(\alpha)}{4 \cos\left(\frac{\theta_{AB}}{2}\right)} (\hat{a} + \hat{b})^2 \mathbf{1} + \frac{E^2 \sin^2(\alpha)}{\sin^2(\theta_{AB})} (\hat{a} \times \hat{b})^2 \mathbf{1} \\
&= \frac{E^2 \cos^2(\alpha)}{4 \cos\left(\frac{\theta_{AB}}{2}\right)} 4 \cos\left(\frac{\theta_{AB}}{2}\right) \mathbf{1} + \frac{E^2 \sin^2(\alpha)}{\sin^2(\theta_{AB})} \sin^2(\theta_{AB}) \mathbf{1} \\
&= E^2 \mathbf{1},
\end{aligned} \tag{A6}$$

therefore, $\langle H_{\text{sub-opt}}^2 \rangle$ becomes

$$\begin{aligned}
\langle H_{\text{sub-opt}}^2 \rangle &= \text{tr} \left[\left(\frac{\mathbf{1} + \hat{a} \cdot \boldsymbol{\sigma}}{2} \right) E^2 \mathbf{1} \right] \\
&= \text{tr} \left(\frac{E^2}{2} \mathbf{1} \right) \\
&= E^2.
\end{aligned} \tag{A7}$$

In conclusion, substituting Eqs. (A4) and (A7) into Eq. (A1), the energy uncertainty ΔE becomes

$$\Delta E = \Delta E(\alpha) \stackrel{\text{def}}{=} E \sqrt{1 - \cos^2(\alpha) \cos^2\left(\frac{\theta_{AB}}{2}\right)}. \tag{A8}$$

The derivation of Eq. (A8) ends our discussion here.

Appendix B: Calculation of κ_{AC}^2

In this Appendix, we introduce the essential elements yielding the notion of curvature coefficient κ_{AC}^2 of a quantum evolution [32, 33]. In particular, this discussion leads to the expression for κ_{AC}^2 in Eq. (35).

Assume to consider a time-varying Hamiltonian evolution specified by the Schrödinger equation $i\hbar\partial_t |\psi(t)\rangle = H(t) |\psi(t)\rangle$, where the normalized quantum state $|\psi(t)\rangle$ belongs to an arbitrary N -dimensional complex Hilbert space \mathcal{H}_N . Usually, $|\psi(t)\rangle$ satisfies $\langle \psi(t) | \dot{\psi}(t) \rangle = (-i/\hbar) \langle \psi(t) | H(t) | \psi(t) \rangle \neq 0$. From the state $|\psi(t)\rangle$, we construct the parallel transported unit state vector $|\Psi(t)\rangle \stackrel{\text{def}}{=} e^{i\beta(t)} |\psi(t)\rangle$ with the phase $\beta(t)$ being such that $\langle \Psi(t) | \dot{\Psi}(t) \rangle = 0$. Notice that $i\hbar |\dot{\Psi}(t)\rangle = [H(t) - \hbar\dot{\beta}(t)] |\Psi(t)\rangle$. Then, the condition $\langle \Psi(t) | \dot{\Psi}(t) \rangle = 0$ is identical to having $\beta(t)$ equal to

$$\beta(t) \stackrel{\text{def}}{=} \frac{1}{\hbar} \int_0^t \langle \psi(t') | H(t') | \psi(t') \rangle dt'. \tag{B1}$$

Therefore, the state vector $|\Psi(t)\rangle$ becomes

$$|\Psi(t)\rangle = e^{(i/\hbar) \int_0^t \langle \psi(t') | H(t') | \psi(t') \rangle dt'} |\psi(t)\rangle, \tag{B2}$$

and fulfills the evolution equation $i\hbar \left| \dot{\Psi}(t) \right\rangle = \Delta H(t) |\Psi(t)\rangle$ with $\Delta H(t) \stackrel{\text{def}}{=} H(t) - \langle H(t) \rangle$. As mentioned in Ref. [33], the speed $v(t)$ of a quantum evolution is not constant when the Hamiltonian changes in time. Specifically, $v(t)$ satisfies $v^2(t) = \left\langle \dot{\Psi}(t) \left| \dot{\Psi}(t) \right\rangle = \left\langle (\Delta H(t))^2 \right\rangle / \hbar^2$. For convenience, we present the arc length $s = s(t)$ defined in terms of $v(t)$ as

$$s(t) \stackrel{\text{def}}{=} \int_0^t v(t') dt', \quad (\text{B3})$$

where $ds = v(t)dt$, that is, $\partial_t = v(t)\partial_s$. Lastly, introducing the adimensional operator $\Delta h(t) \stackrel{\text{def}}{=} \Delta H(t) / [\hbar v(t)] = \Delta H(t) / \sqrt{\left\langle (\Delta H(t))^2 \right\rangle}$, the normalized tangent vector $|T(s)\rangle \stackrel{\text{def}}{=} \partial_s |\Psi(s)\rangle = |\Psi'(s)\rangle$ reduces to $|T(s)\rangle = -i\Delta h(s) |\Psi(s)\rangle$. We point out that $\langle T(s) | T(s) \rangle = 1$ by construction and, additionally, $\partial_s \langle \Delta h(s) \rangle = \langle \Delta h'(s) \rangle$. Interestingly, this latter relation remains valid for arbitrary powers of differentiation. For instance, to the second power, we find $\partial_s^2 \langle \Delta h(s) \rangle = \langle \Delta h''(s) \rangle$. We can generate $|T'(s)\rangle \stackrel{\text{def}}{=} \partial_s |T(s)\rangle$ from the tangent vector $|T(s)\rangle = -i\Delta h(s) |\Psi(s)\rangle$. More explicitly, we get $|T'(s)\rangle = -i\Delta h(s) |\Psi'(s)\rangle - i\Delta h'(s) |\Psi(s)\rangle$ where, in general,

$$\langle T'(s) | T'(s) \rangle = \left\langle (\Delta h'(s))^2 \right\rangle + \left\langle (\Delta h(s))^4 \right\rangle - 2i \text{Re} \left[\left\langle \Delta h'(s) (\Delta h(s))^2 \right\rangle \right] \neq 1. \quad (\text{B4})$$

We are now ready to introduce the curvature coefficient for quantum evolutions emerging from time-varying Hamiltonians. As a matter of fact, having presented the vectors $|\Psi(s)\rangle$, $|T(s)\rangle$, and $|T'(s)\rangle$, we can finally define the curvature coefficient $\kappa_{\text{AC}}^2(s) \stackrel{\text{def}}{=} \left\langle \tilde{N}_*(s) \left| \tilde{N}_*(s) \right\rangle$ with $|\tilde{N}_*(s)\rangle \stackrel{\text{def}}{=} P^{(\Psi)} |T'(s)\rangle$, $P^{(\Psi)} \stackrel{\text{def}}{=} I - |\Psi(s)\rangle \langle \Psi(s)|$, and “I” being the identity operator in \mathcal{H}_N . As reported in Refs. [32, 33], the subscript “AC” stands for Alsing and Cafaro. Note that the curvature coefficient $\kappa_{\text{AC}}^2(s)$ can be rewritten as

$$\kappa_{\text{AC}}^2(s) \stackrel{\text{def}}{=} \|D |T(s)\rangle\|^2 = \|D^2 |\Psi(s)\rangle\|^2, \quad (\text{B5})$$

with $D \stackrel{\text{def}}{=} P^{(\Psi)} d/ds = (I - |\Psi\rangle \langle \Psi|) d/ds$ and $D |T(s)\rangle \stackrel{\text{def}}{=} P^{(\Psi)} |T'(s)\rangle$ denoting the covariant derivative [17, 56, 57]. We observe that the curvature coefficient $\kappa_{\text{AC}}^2(s)$ in Eq. (B5) equals the magnitude squared of the second covariant derivative of the state vector $|\Psi(s)\rangle$ used to construct the quantum Schrödinger trajectory in projective Hilbert space. To be crystal clear, we remark that $|\tilde{N}_*(s)\rangle$ is a vector that is neither orthogonal to the vector $|T(s)\rangle$ nor normalized to one. On the contrary, despite being unnormalized, $|\tilde{N}(s)\rangle \stackrel{\text{def}}{=} P^{(T)} P^{(\Psi)} |T'(s)\rangle$ is orthogonal to $|T(s)\rangle$. Lastly, $|N(s)\rangle \stackrel{\text{def}}{=} |\tilde{N}(s)\rangle / \sqrt{\left\langle \tilde{N}(s) \left| \tilde{N}(s) \right\rangle}$ is a normalized vector which is orthogonal to $|T(s)\rangle$. Summing up, $\{|\Psi(s)\rangle, |T(s)\rangle, |N(s)\rangle\}$ is the set of three orthonormal vectors needed to specify the curvature coefficient of a quantum evolution. Note that, although \mathcal{H}_N can possess arbitrary dimension as a complex space, we limit our attention to the three-dimensional complex subspace generated by $\{|\Psi(s)\rangle, |T(s)\rangle, |N(s)\rangle\}$. Nevertheless, our working assumption agrees with the classical geometric viewpoint according to which the curvature and torsion coefficients can be regarded as the lowest and second-lowest, respectively, members of a family of generalized curvatures functions [58]. Particularly, for curves in higher-dimensional spaces, this sound geometric perspective demands a set of m orthonormal vectors to construct $(m-1)$ -generalized curvature functions [58].

In general, the direct evaluation of the time-dependent curvature coefficient $\kappa_{\text{AC}}^2(s)$ in Eqs. (B5) by means of the projection operators formalism is challenging. The difficulty is caused by the fact that, in analogy to what happens in the classical case of space curves in \mathbb{R}^3 [59], there exist two main drawbacks when reparameterizing a quantum curve by its arc length s . Firstly, we may be unable to evaluate in closed form $s(t)$ in Eq. (B3). Secondly, even if we are capable of getting $s = s(t)$, we may not be able to invert this relation and, thus, arrive at $t = t(s)$ needed to obtain $|\Psi(s)\rangle \stackrel{\text{def}}{=} |\Psi(t(s))\rangle$. To avoid these challenges, we can rewrite $\kappa_{\text{AC}}^2(s)$ in Eq. (B5) by means of expectation values defined with respect to the state $|\Psi(t)\rangle$ (or, alternatively, with respect to $|\psi(t)\rangle$) that can be computed without the relation $t = t(s)$. For ease of notation, in the following discussion, we shall avoid making any explicit reference to the s -dependence of the variety of operators and expectation values being considered. For instance, $\Delta h(s)$ will appear as Δh . After some algebra, we get

$$|\tilde{N}_*\rangle = - \left\{ \left[(\Delta h)^2 - \left\langle (\Delta h)^2 \right\rangle \right] + i [\Delta h' - \langle \Delta h' \rangle] \right\} |\Psi\rangle, \quad (\text{B6})$$

with $\Delta h' = \partial_s (\Delta h) = [\partial_t (\Delta h)] / v(t)$. To calculate $\kappa_{\text{AC}}^2(s) \stackrel{\text{def}}{=} \left\langle \tilde{N}_*(s) \left| \tilde{N}_*(s) \right\rangle$, it is useful to employ the Hermitian operator $\hat{\alpha}_1 \stackrel{\text{def}}{=} (\Delta h)^2 - \left\langle (\Delta h)^2 \right\rangle$ and the anti-Hermitian operator $\hat{\beta}_1 \stackrel{\text{def}}{=} i [\Delta h' - \langle \Delta h' \rangle]$ where $\hat{\beta}_1^\dagger = -\hat{\beta}_1$. Then,

$|\tilde{N}_*\rangle = -(\hat{\alpha}_1 + \hat{\beta}_1)|\Psi\rangle$ and $\langle \tilde{N}_*(s) | \tilde{N}_*(s) \rangle$ equals $\langle \hat{\alpha}_1^2 \rangle - \langle \hat{\beta}_1^2 \rangle + \langle [\hat{\alpha}_1, \hat{\beta}_1] \rangle$ with $[\hat{\alpha}_1, \hat{\beta}_1] \stackrel{\text{def}}{=} \hat{\alpha}_1\hat{\beta}_1 - \hat{\beta}_1\hat{\alpha}_1$ denoting the quantum commutator of $\hat{\alpha}_1$ and $\hat{\beta}_1$. Note that the expectation value $\langle [\hat{\alpha}_1, \hat{\beta}_1] \rangle$ belongs to \mathbb{R} given that $[\hat{\alpha}_1, \hat{\beta}_1]$ is a Hermitian operator. This is due to the fact that $\hat{\alpha}_1$ and $\hat{\beta}_1$ represent Hermitian and anti-Hermitian operators, respectively. Exploiting the definitions of $\hat{\alpha}_1$ and $\hat{\beta}_1$, we obtain $\langle \hat{\alpha}_1^2 \rangle = \langle (\Delta h)^4 \rangle - \langle (\Delta h)^2 \rangle^2$, $\langle \hat{\beta}_1^2 \rangle = -\langle (\Delta h')^2 \rangle + \langle \Delta h' \rangle^2$, and $\langle [\hat{\alpha}_1, \hat{\beta}_1] \rangle = i\langle [(\Delta h)^2, \Delta h'] \rangle$. Observe that $\langle [(\Delta h)^2, \Delta h'] \rangle$ is purely imaginary given that $[(\Delta h)^2, \Delta h']$ is an anti-Hermitian operator. For completeness, we remark that $[(\Delta h)^2, \Delta h']$ is generally not a null operator. As a matter of fact, $[(\Delta h)^2, \Delta h'] = \Delta h [\Delta h, \Delta h'] + [\Delta h, \Delta h'] \Delta h$ with $[\Delta h, \Delta h'] = [H, H']$. Then, focusing on time-varying qubit Hamiltonians of the form $H(s) \stackrel{\text{def}}{=} \mathbf{h}(s) \cdot \boldsymbol{\sigma}$, the commutator $[H, H'] = 2i(\mathbf{h} \times \mathbf{h}') \cdot \boldsymbol{\sigma}$ is not equal to zero given that the vectors \mathbf{h} and \mathbf{h}' are not generally collinear. Obviously, $\boldsymbol{\sigma}$ is the vector operator whose components are defined by the Pauli operators σ_x , σ_y , and σ_z . Finally, a computationally useful expression for the curvature coefficient $\kappa_{\text{AC}}^2(s)$ in Eq. (B5) in an arbitrary time-varying framework becomes

$$\kappa_{\text{AC}}^2(s) = \langle (\Delta h)^4 \rangle - \langle (\Delta h)^2 \rangle^2 + \langle (\Delta h')^2 \rangle - \langle \Delta h' \rangle^2 + i\langle [(\Delta h)^2, \Delta h'] \rangle. \quad (\text{B7})$$

From Eq. (B7), we realize that when the Hamiltonian H does not depend on time, $\Delta h'$ reduces to the null operator and we recuperate the stationary limit $\langle (\Delta h)^4 \rangle - \langle (\Delta h)^2 \rangle^2$ of $\kappa_{\text{AC}}^2(s)$ [32].

The formulation of $\kappa_{\text{AC}}^2(s)$ in Eq. (B7) is acquired by means of an approach that relies upon the calculation of expectation values which, in turn, demand the knowledge of the state vector $|\psi(t)\rangle$ satisfying the time-dependent Schrödinger evolution equation. As remarked in Ref. [33], such expectation-values approach yields an insightful statistical interpretation for $\kappa_{\text{AC}}^2(s)$. Simultaneously, however, this approach does not possess a neat geometric significance. Driven by this shortfall and limiting our attention to time-varying Hamiltonians and two-level quantum systems, it is possible to obtain a closed-form expression for the curvature coefficient for a curve traced out by a single-qubit quantum state that changes under the action of a general time-dependent Hamiltonian. The curvature coefficient κ_{AC}^2 can be fully expressed in terms of only two real three-dimensional vectors with a transparent geometrical interpretation. Namely, the two vectors are the Bloch vector $\mathbf{a}(t)$ and the magnetic field vector $\mathbf{h}(t)$. While the former vector defines the density operator $\rho(t) = |\psi(t)\rangle \langle \psi(t)| \stackrel{\text{def}}{=} [I + \mathbf{a}(t) \cdot \boldsymbol{\sigma}] / 2$, the latter characterizes the time-varying (traceless) Hamiltonian $H(t) \stackrel{\text{def}}{=} \mathbf{h}(t) \cdot \boldsymbol{\sigma}$. Following the extended analysis presented in Ref. [33], we obtain

$$\kappa_{\text{AC}}^2(\mathbf{a}, \mathbf{h}) = 4 \frac{(\mathbf{a} \cdot \mathbf{h})^2}{\mathbf{h}^2 - (\mathbf{a} \cdot \mathbf{h})^2} + \frac{[\mathbf{h}^2 \dot{\mathbf{h}}^2 - (\mathbf{h} \cdot \dot{\mathbf{h}})^2] - [(\mathbf{a} \cdot \dot{\mathbf{h}}) \mathbf{h} - (\mathbf{a} \cdot \mathbf{h}) \dot{\mathbf{h}}]^2}{[\mathbf{h}^2 - (\mathbf{a} \cdot \mathbf{h})^2]^3} + 4 \frac{(\mathbf{a} \cdot \mathbf{h}) [\mathbf{a} \cdot (\mathbf{h} \times \dot{\mathbf{h}})]}{[\mathbf{h}^2 - (\mathbf{a} \cdot \mathbf{h})^2]^2}. \quad (\text{B8})$$

The derivation of κ_{AC}^2 in Eq. (B8) serves as a valuable tool for computational analysis in qubit systems. Furthermore, it presents a lucid geometric interpretation of the curvature of a quantum evolution by means of the (normalized unitless) Bloch vector \mathbf{a} and the (usually unnormalized, with $[\mathbf{h}]_{\text{MKSA}} = \text{joules} = \text{sec}^{-1}$ when putting $\hbar = 1$) magnetic field vector \mathbf{h} . Our discussion concludes with the derivation of Eq. (B8).